



HAL
open science

Modeling of excited state potential energy surfaces with the Bethe–Salpeter equation formalism: The 4-(dimethylamino)benzotrile twist

Iryna Knysh, Ivan Duchemin, Xavier Blase, Denis Jacquemin

► To cite this version:

Iryna Knysh, Ivan Duchemin, Xavier Blase, Denis Jacquemin. Modeling of excited state potential energy surfaces with the Bethe–Salpeter equation formalism: The 4-(dimethylamino)benzotrile twist. *The Journal of Chemical Physics*, 2022, 157 (19), pp.194102. 10.1063/5.0121121 . hal-03854780

HAL Id: hal-03854780

<https://cnrs.hal.science/hal-03854780v1>

Submitted on 16 Nov 2022

HAL is a multi-disciplinary open access archive for the deposit and dissemination of scientific research documents, whether they are published or not. The documents may come from teaching and research institutions in France or abroad, or from public or private research centers.

L'archive ouverte pluridisciplinaire **HAL**, est destinée au dépôt et à la diffusion de documents scientifiques de niveau recherche, publiés ou non, émanant des établissements d'enseignement et de recherche français ou étrangers, des laboratoires publics ou privés.

Modelling of excited state potential energy surfaces with the Bethe-Salpeter equation formalism: The 4-(dimethylamino)benzonitrile twist

Iryna Knysh,¹ Ivan Duchemin,² Xavier Blase,³ and Denis Jacquemin¹

¹*Nantes Université, CNRS, CEISAM UMR 6230, F-44000 Nantes, France*

²*Université Grenoble Alpes, CEA, IRIG-MEM-L_Sim, 38054 Grenoble, France*

³*Université Grenoble Alpes, Centre National de la Recherche Scientifique, Institut Néel, F-38042 Grenoble, France*

(*Electronic mail: Denis.Jacquemin@univ-nantes.fr)

(*Electronic mail: xavier.blase@neel.cnrs.fr)

We present a benchmark study of excited state potential energy surfaces (PES) using the many-body Green's function GW and Bethe-Salpeter equation (BSE) formalisms, coupled cluster methods, as well as Time-Dependent Density Functional Theory. More specifically, we investigate the evolution of the two lowest excited states of 4-(dimethylamino)benzonitrile (DMABN) upon the twisting of the amino group, a paradigmatic system for dual fluorescence and excited-state benchmarks. Our results demonstrate that the BSE/ GW approach is able to reproduce the correct topology of excited state PES upon geometry changes in both gas and condensed phases. The vertical transition energies predicted by BSE/ GW are indeed in good agreement with coupled cluster values including triples. The BSE approach ability to include both linear response and state-specific solvent corrections further enables it to accurately describe the solvatochromisms of both excited states during the twisting of DMABN. This contribution stands as one of the first proof-of-concept that BSE/ GW PES should be accurate in cases for which TD-DFT struggles, including the central case of systems embedded in a dielectric environment.

I. INTRODUCTION

The fascinating phenomenon of dual fluorescence, firstly reported by Lippert and co-workers¹ for DMABN, was the subject of many studies during the last decades.² In DMABN, dual fluorescence leads to the appearance of an unexpected low-energy band in the emission spectra, whose position and intensity depend on the solvent polarity and temperature. In non-polar solvents, only one fluorescence band originating from the 1L_b -type state, often referred to as local excited (LE) state, is present. In addition, in polar solvents, a second redshifted band assigned to the 1L_a -type state presenting an intramolecular charge transfer (CT) nature can be observed. Experimentally it was shown that only the LE state can be populated through absorption.³ In order to explain the fluorescence from the CT state different theories and models were proposed.⁴⁻⁹ Among them the most commonly accepted is the twisted intramolecular charge transfer (TICT) model.^{2,4,9} According to it, the CT fluorescence occurs after rotation of the amino group in the excited state (ES), making it perpendicular to the benzonitrile ring (see Figure 1).

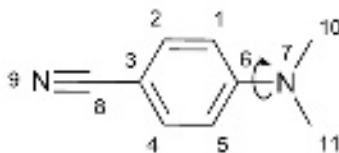


FIG. 1. Structure of DMABN molecule with numbering of the atoms and representation of the twist responsible for TICT.

The availability of efficient and reliable theoretical tools is an important factor to rationalize emission processes. More specifically, in the case of TICT molecules, the possibility of probing the shape of the ES potential energy surfaces (PES) upon twisting is a key to explain the abnormal fluorescence. Due to the limitations of excited state geometry optimizations in existing quantum chemical codes, the first high-level theoretical studies of DMABN have been done using the complete active space self-consistent field (CASSCF) and CAS perturbation theory to second order (CASPT2) methods on the geometries optimized at the Hartree Fock (HF) and configuration interaction singles (CIS) levels of theory.^{8,10} Although CASPT2 reproduced the correct evolution of the excited state surfaces, CASSCF provided an incorrect description of the PES due to the lack of dynamic electron correlation.¹⁰ Implementation of the analytical gradients for the second-order coupled cluster (CC2)¹¹⁻¹⁴ method allowed to perform the relaxed PES studies for the two lowest singlet excited states of DMABN upon twisting (in gas phase).¹⁵ This work was the first coupled

cluster work supporting the TICT hypothesis, as CC2 shows a remarkable lowering of the CT state energies upon twisting.

Including the solvent effects is also essential to reproduce experimental outcomes, especially the emergence of dual fluorescence when going from non-polar to polar solvents. The available theoretical solvation models can be divided into two groups: implicit (the solvent is represented as a continuous medium) and explicit (each solvent molecule is explicitly modeled). Although the latter models provide an improved description of solvent-solute specific interactions, they are much more computationally demanding than the former ones. Continuum approaches like the well-known polarizable continuum model (PCM)¹⁶ advantageously allow to estimate solvent effects at a very low cost. Nevertheless several complications arise when accounting for the solvent effects during the ES processes. In the case of vertical absorption only the electrons of the solvent can respond to the change of density of the solute, while the positions of the solvent nuclei remain "frozen", *i.e.*, equilibrated with the ground state (GS) solute density. This corresponds to a non-equilibrium regime which is adequate for computing the solvent response related to electronic transitions. In contrast, during slower processes the solvent and solute have enough time to mutually polarize, and an equilibrium regime can be reached, *i.e.*, both the electrons and nuclei of the solvent are equilibrated with the ES density. Additionally, in implicit solvation models the ES energies can be computed using either the linear response (LR) or state-specific (SS) formalisms.¹⁷ The former one captures the solvent response through the transition density between the two states while the latter one computes the solvent effects as a response to the ES total density. The relative magnitude of the LR and SS corrections depends on the nature of the considered state, and it has been advocated by several authors that both effects need to be considered for reaching the best accuracy.^{18–21} Despite the above-listed challenges in the description of ES properties in condensed phase, implicit inclusion of solvent effects is now possible in numerous quantum-chemical codes.

Notably, theoretical studies of DMABN spectral properties in solution are available. One of the first works on the solvent effect was done by Mennucci *et al.* using the multireference perturbed CI polarizable continuum model and the PCM solvation scheme.²² In this work two mechanisms for dual fluorescence of DMABN have been studied, namely PICT (corresponding to a planar ICT, wagging motion of the amino group)⁶ and TICT. Based on the obtained results they concluded that the TICT model is suited to explain the dual fluorescence phenomenon occurring in DMABN solvated in a polar solvent. Latter, Georgieva *et al.*²³ used the multireference configuration interaction (MRCI) and algebraic diagrammatic construction (ADC) methods to study the mechanisms

leading to dual fluorescence. They were able to account for the solvent (acetonitrile) effects on the excited state energies by using the conductor-like screening model (COSMO).²⁴ They found that the CT state of DMABN is characterized by a large charge separation which results in a more stable CT state minimum (than LE) in polar solvents. Their findings therefore supports the TICT model, where the twisted CT state is responsible for the second emission band of DMABN. Later, Mewes and co-workers²⁵ implemented a SS continuum model for the second and third order ADC methods. Although they were able to achieve an excellent agreement with the experimental data for the LE fluorescence, this SS-PCM-ADC approach did not led to a perfect match with experimental measurements of the CT state energies in non-polar solvents. Finally, Caricato recently presented a coupled cluster with singles and doubles (CCSD) study combined with the LR approach of the perturbation theory energy and singles-T density (PTES)^{26,27} and its application to the DMABN in both polar and non-polar solvents.²⁸ Despite reproducing in most cases the experimental trends, the LR formalism, as expected, was unable to reproduce the lowering of the CT state energies in the polar solvents. In contrast, the SS formalism^{29,30} appears to greatly overestimate the solvent polarization effect for the CT state, similarly to the SS-PCM-ADC findings.²⁵

The above-discussed high level theories are typically accurate in predicting the excited state energies, but they remain highly expensive and their applications are limited to small systems. In consequence, the most frequently used method for the ES calculations remains Time-Dependent Density Functional Theory (TD-DFT).^{31,32} TD-DFT was also employed for studying the abnormal fluorescence from the CT state of DMABN.^{33–35} However, some of these results are biased by the well-known incorrect TD-DFT description of charge-transfer states.^{36,37} Notably, Wiggins *et al.*³⁸ published a benchmark study of the modelling the excited states PES of DMABN with TD-DFT. Using a previously developed diagnostic tool to evaluate the degree of spatial overlap between the occupied and virtual orbitals involved in an excitation,³⁹ they rationalized the errors obtained with different DFT exchange-correlation functionals (XCFs). In particular they showed that during twisting the spatial orbital overlap is getting smaller and this results in the collapse of the excited state PES for both generalized gradient approximations (GGAs) and global hybrid XCFs. A qualitatively correct evolution of the PES can be restored using range-separated hybrids (RSH), like CAM-B3LYP.⁴⁰ However, the use of RSH usually results in a slight overestimation of the LE transition.⁴¹ Moreover, in the case of DMABN, the nature of the CT and LE states are mixed during the twist and the CAM-B3LYP energies are somehow overestimated as compared to CC2 reference values used by Wiggins *et al.*³⁸

Alternatively, the Bethe-Salpeter equation (BSE) formalism^{42–44} has recently appeared as a valuable compromise between TD-DFT and wavefunction techniques for the study of large dyes and fluorophores. The BSE formalism is based on the time-ordered one-body Green's function (G) many-body perturbation theories and takes as an input the electronic energy levels (or quasiparticle energies) and screened Coulomb potential (W) generated with the GW approach.⁴⁵ In particular, previous works showed that BSE/ GW correctly predicts the energies of CT transitions while being equally good for describing valence and Rydberg excitations.^{46–51} Furthermore, the problematic modelling of the excitation energies of the cyanine derivatives with TD-DFT can be resolved using the BSE formalism.⁵² By performing a partially self-consistent scheme (ev GW), where only KS eigenvalues are updated (but the eigenvectors are frozen), one can both improve the quality of quasiparticle energies^{53–55} and wash out most of the starting point dependency, *i.e.*, BSE/ev GW energies are much less dependent on the selected XCF than TD-DFT's.^{51,56} Such an improvement of the quasiparticle energies, and the correlated improvement in the BSE excitation energies,⁵⁷ is particularly important when starting with Kohn-Sham eigenstates generated with a reduced amount of exact exchange. Additionally, the BSE approach naturally allows for the simultaneous account of both LR and SS solvent effects when combined, e.g., with the PCM,²⁰ a paramount advantage when dealing with the effect of a dielectric environment. However, a clear drawback of the BSE/ GW approach is the lack of analytical gradients within efficient linear response techniques such as the Z -vector approach.⁵⁸ Pioneering studies on a limited set of small molecules (carbon monoxide, acetone, acrolein, and methylene-cyclopropene) concluded on the promising accuracy of the BSE/ GW gradients,^{59,60} inviting to keep exploring BSE/ GW excited state energy surfaces in the case of complex systems for which TD-DFT may face difficulties and, further, in the crucial case of solvated systems.

II. COMPUTATIONAL DETAILS

Gas Phase. Two sets of gas-phase geometries are used in this study: CCSD(T)-interpolated and (EOM)-CCSD-optimized applying the frozen-core approximation in both cases. We consider here structures with a twist angle between the dimethylamino group (NMe_2) and the phenyl ring going from 0° to 90° by step of 10° (see Figure 1). In the first set, the ground state (GS) structures with 0° and 90° angles have been optimized at the Coupled Cluster Single and Double including non-iterative Triple [CCSD(T)]⁶¹ level with the cc-pVTZ atomic basis set using the CFOUR2.1

program.^{62,63} The C_{2v} symmetry of these two structures was enforced during calculations, and these two geometries already appeared in one of our previous work.⁶⁴ Subsequently, the intermediate geometries were simply interpolated using 10° step. In the second set, the GS structures were allowed to fully relax while keeping the 1-6-7-10 and 5-6-7-11 (see Figure 1) dihedral angles frozen. The two lowest excited states (LE and CT) were optimized in the same way as a ground state, *i.e.*, constraining only the twist angles and enforcing the C_2 symmetry. These calculations were done with CCSD/cc-pVDZ and the Equation of Motion (EOM)-CCSD/cc-pVDZ levels of theory for the GS and ES, respectively, using Gaussian 16 program.⁶⁵ *Tight* convergence criteria were used during the geometry optimization. Cartesian coordinates for both sets of geometries are given in the Supplementary Materials (SM).

For the comparisons with experiment in Section IV we optimized of the GS, LE, and CT minima structures using the (EOM)-CCSD/cc-pVDZ level of theory implemented in Gaussian 16. The frequency analysis confirmed that all optimized structures are true minima. The obtained geometries are similar to the ones published by Caricato.²⁸ We provide the Cartesian coordinates in the SM.

The vertical transition energies were determined on interpolated geometries using various EOM-CC methods, *i.e.*, CC2,¹¹⁻¹⁴ CCSD,^{61,66-69} CCSD(T)(a)*,⁷⁰ and third-order CC (CC3).^{71,72} Dunning's correlation consistent basis sets (cc-pVDZ and cc-pVTZ)⁷³⁻⁷⁷ were employed for this purpose. These calculations were achieved with the CFOUR2.1 program. DFT, TD-DFT and BSE/evGW results on these geometries were obtained using the following XCFs: BLYP,^{78,79} B3LYP,^{78,80} BHLYP,⁸⁰ CAM-B3LYP,⁴⁰ PBE,⁸¹ and PBE0,^{81,82} and the cc-pVTZ basis set. TD-DFT calculations were performed with the Gaussian 16 program, while BSE/evGW calculations were conducted with the BEDEFT code,⁸³ a rewriting and extension of the FIESTA code,^{53,56,84} on the basis of input Kohn-Sham eigenstates obtained with the ORCA 5.0 program. We corrected the 14 highest occupied and the 20 lowest unoccupied eigenvalues at the evGW level. BSE/evGW calculations were performed including all occupied/virtual states in the construction of the susceptibility operators and of the optical excitations. The dynamics of the GW operator is treated exactly using a recently developed analytic continuation approach⁸³ and the Coulomb-fitting resolution of the identity⁸⁵ is adopted with the corresponding cc-pVTZ-RI auxiliary basis set.⁸⁶ BSE calculations are performed beyond the Tamm-Dancoff approximation, *i.e.*, with the full matrix.⁸⁷⁻⁸⁹ Single-point energy calculations on the (EOM)-CCSD optimized set of geometries of GS, LE, and CT electronic states were achieved with the cc-pVTZ basis set using DFT, TD-DFT, BSE/evGW,

and CCSD levels of theory with the same codes as above.

Solution. Solvent effects were accounted by using the PCM model¹⁶ choosing n-hexane (later referred as hexane) and acetonitrile (MeCN) as solvents. (EOM)-CCSD-optimized sets of geometries for the ground and excited states were obtained at the (EOM)-CCSD/cc-pVDZ level of theory with the perturbation theory energy and density (PTED)^{90,91} solvation scheme (SS-PTED^{29,30} for ES states) keeping the constraints on the twist angles and enforcing C_2 symmetry. As a result, two new sets of geometries were obtained - Hexane-PTED-(EOM)-CCSD-optimized and MeCN-PTED-(EOM)-CCSD-optimized. The equilibrium solvation regime was used during the geometry optimization. As in the gas phase we used *tight* convergence criteria during the geometry optimization. The geometry optimization of the GS minima in acetonitrile was performed at the PTED-CCSD/cc-pVDZ level of theory using the Gaussian 16 program. The frequency analysis confirmed the absence of imaginary frequencies. We provide the Cartesian coordinates in the SM.

The vertical transition energies were computed on PTED-CCSD-optimized sets of geometries in the corresponding solvent using both the LR and SS formalisms at the PTED-EOM-CCSD/cc-pVTZ level of theory. We applied non-equilibrium regime for computing the transition energies. At the TD-DFT level we used LR,^{92,93} cLR (known as CorrectedLR),⁹⁴ and cLR²,²¹ solvent models with the B3LYP and CAM-B3LYP XCFs and cc-pVTZ basis set. cLR and cLR² are SS approaches, the latter including both the LR and SS corrections.²¹ Default PCM settings of Gaussian 16 program have been used for these calculations.

The merging of the *GW* and Bethe-Salpeter formalisms with the PCM approach is described in details in Refs. 20 and 95. In a nutshell, the standard gas phase *GW* and subsequent BSE calculations can be modified to account for the response of a dielectric environment to an electronic excitation on the solute by dressing the bare Coulomb potential with the so-called reaction field:

$$v(\mathbf{r}, \mathbf{r}') \implies v(\mathbf{r}, \mathbf{r}') + v^{\text{reac}}(\mathbf{r}, \mathbf{r}')$$

where $v^{\text{reac}}(\mathbf{r}, \mathbf{r}')$ is the field generated in (\mathbf{r}') by the rearrangement of charges in the dielectric environment induced by a unit charge variation in (\mathbf{r}) . In the PCM model, such charge rearrangements are generated at the surface of the dielectric cavity. This renormalization of the bare Coulomb potential leads further to a dressed screened Coulomb potential W through the associated Dyson equation: $W = v + v\chi_0 W$, with χ_0 being the solute independent-electron susceptibility. As a result, the *GW* energy levels (or quasiparticle energies) and the BSE neutral excitations properly include the effect of the solvent. As shown in Ref. 20, both state-specific (SS) and linear-response (LR)

contributions are automatically accounted for. The LR correction is associated with the dressing of the bare Coulomb potential matrix elements in the BSE two-body (electron-hole) Hamiltonian, while the SS contribution hinges on the modification of the screened Coulomb potential W that affects the GW quasiparticle energies and the screened electron-hole interaction.

The PCM- GW calculations are performed at the proper non-equilibrium level with the environment slow (nuclear) and fast (electronic) degrees of freedom accounted for at the input PCM-DFT level, while retaining only the fast dielectric response when screening the solute electronic excitations.⁹⁵ While the solvent dielectric constant is, on general grounds, frequency-dependent, the PCM reaction field used in the BSE/ GW calculations is taken to be static and equal to its low-frequency value in the optical range. This is consistent with the restriction of the screened Coulomb potential to its low frequency limit in the standard BSE approach, an approximation analogous to using a static kernel in TD-DFT. The solvent dielectric response is based on cavities generated from the superposition of atom-centered spheres, using the scaled universal force field⁹⁶ van der Waal's radii with a 1.1 scaling factor consistently with the default in Gaussian09. The present IEF-PCM with BSE/ GW (later referred as PCM-BSE/ev GW /B3LYP) implementation follows the double layer surface potential approach^{20,95} previously tested within the FIESTA implementation. During the solvent calculations, 10 occupied and 10 virtual MOs were corrected at the GW level.

Additionally, we also determined the CT parameters using Le Bahers metric,^{97,98} namely the CT distance (D_{CT}), that allows to define the spatial separation between the electron and the hole associated to a given transition, the amount of transferred charge from the ground to the excited states (q_{CT}), and the variation of dipole moment between the ground and the excited states (μ_{CT}). The above mentioned calculations have been done at LR-PCM-TD-CAM-B3LYP/cc-pVTZ level of theory in hexane and acetonitrile using the Gaussian 16 program.

In the discussion of the results we present the excited state PES as ES relative energies *versus* twist angle. The ES relative energies were computed as differences between the ES total energy, $E_{ES}(\phi)$, and the GS energy of the untwisted molecule, $E_{GS}(0^\circ)$,

$$\Delta E(\phi) = E_{ES}(\phi) - E_{GS}(0^\circ).$$

The ES total energy for BSE/ GW is calculated as the sum of BSE vertical transition energy and the DFT ground state energy.

III. RESULTS AND DISCUSSION

A. Gas-phase reference values

We first start with the gas phase results obtained on interpolated geometries using various CC methods. We present a highly accurate excited state PES obtained with perturbative triple CC method and the cc-pVTZ basis set in Figure 2a. We additionally provide a comparison between CC3/cc-pVDZ and CCSD(T)(a)*/cc-pVDZ results in the SM (see Figure S1 and Table S1) confirming the quality of the latter method, which is used as a benchmark for the CC2, CCSD, TD-DFT, and BSE/evGW methods. The PESs obtained with CCSD and CC2 methods for the two lowest singlet excited states of DMABN, namely the LE and CT states, are respectively presented in Figures 2b and 2c. Clearly, both methods deliver qualitatively correct PES topologies. In particular, the twisted CT state remains higher in energy than the untwisted LE one, consistently with the absence of a red-shifted TICT band in the gas phase fluorescence spectra.

It is seen that CCSD excited state energies are slightly overestimating the CCSD(T)(a)* ones, a typical trend of CCSD.^{99–101} Quite the opposite is observed for CC2 that underestimates the transition energies and also shifts the crossing point between the LE and CT states to slightly lower dihedral angles. Indeed, this crossing appears between 40° and 50° with CC2, but at 50° with the two other methods. The same trend is found for the vertical absorption energies of both excited states (see Table S2). The differences between CCSD and CCSD(T)(a)* results are more uniform than their CC2 *versus* CCSD(T)(a)* counterparts. Such kind of behaviour for these two CC methods was reported before for intramolecular charge-transfer excitations.⁶⁴

Previously, Köhn and Hättig presented the relaxation of two lowest singlet excited states of DMABN with fixed twist angles and imposing C_2 symmetry using the CC2/TZ2P approach.¹⁵ We also performed such optimizations at the (EOM)-CCSD/cc-pVDZ level and computed energies of both states as well using the larger cc-pVTZ basis set. Our data can be found in Figure S3 and Table S9 in the SM. Relaxation of the geometries with CCSD induces a shift of the crossing point a bit further than 50° (Figures 2b and S3). Furthermore, one can also observe the expected lowering of the relative energies obtained on optimized structures for both excited states. Consistent with previous works,^{15,38} the structural relaxation induces a shallow minimum on the PES of LE state at *ca.* 20° (see Figure S3). This indicates that the LE state minimum is not planar, in agreement with 19° twist angle previously reported at the CC2 level of theory.¹⁵

This is the author's peer reviewed, accepted manuscript. However, the online version of record will be different from this version once it has been copyedited and typeset.
PLEASE CITE THIS ARTICLE AS DOI:10.1063/5.0121121

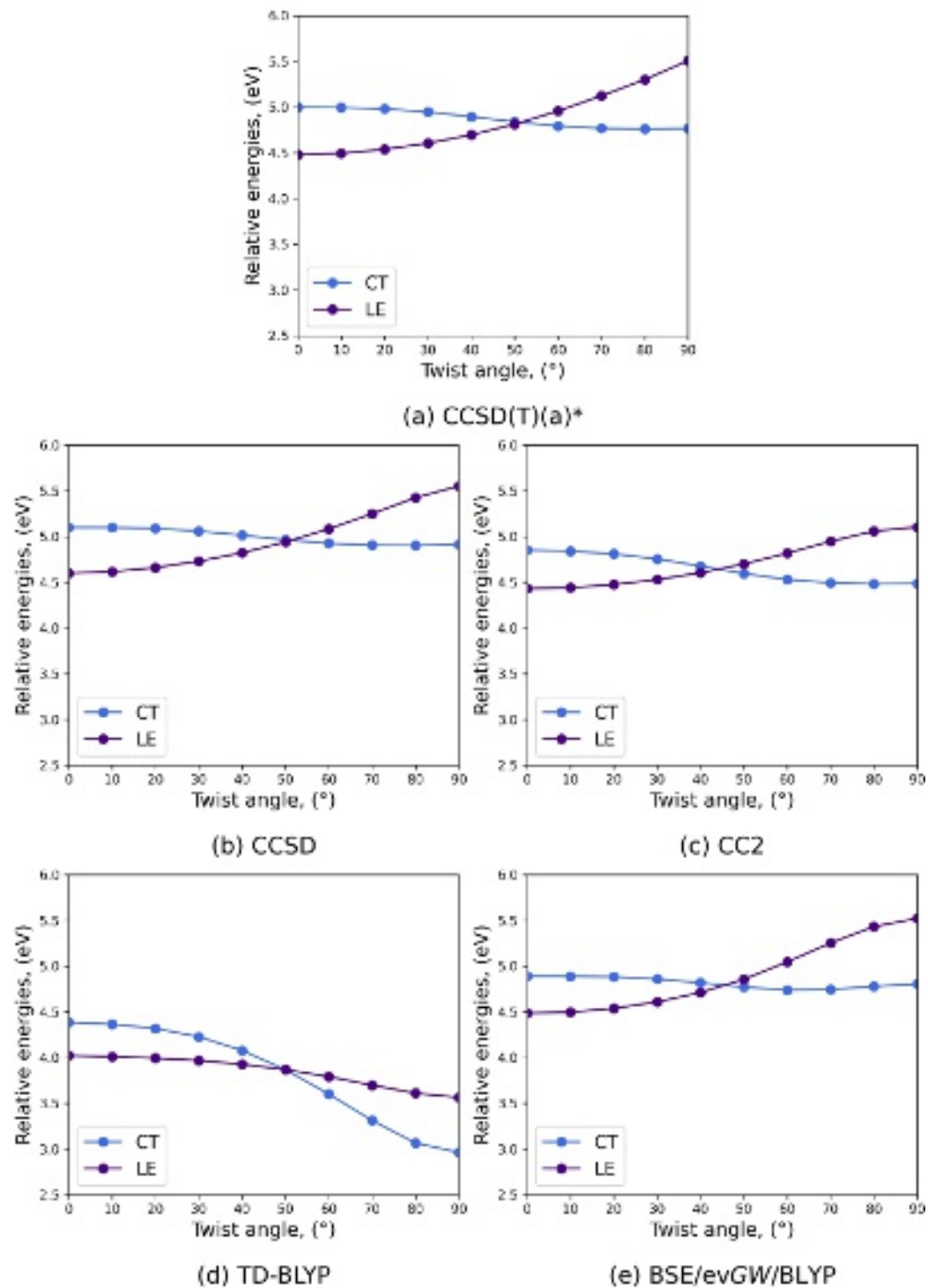


FIG. 2. PES for CT and LE states of DMABN calculated on the CCSD(T)-interpolated geometries at the CCSD(T)(a)*, CCSD, CC2, TD-BLYP, and BSE/evGW/BLYP levels of theory in gas phase using the cc-pVTZ basis set. Relative energies use the GS energy of the untwisted molecule as reference. In the case of the BSE/evGW/BLYP calculations, the GS energy is calculated at the DFT BLYP level.

B. BSE vs TD-DFT

The data obtained on interpolated geometries with BSE/evGW/BLYP and TD-BLYP are presented in Figure 2. As was shown by Wiggins *et al.*³⁸ the use of a GGA XCF (in their case PBE) yields a qualitatively incorrect evolution of the excited state energies along the twist coordinate. One observes the same trends with BLYP in Figure 2d: the CT state relative energies are decreasing both too strongly and too rapidly as the twist increases, whereas the corresponding LE energies are following a lowering trend instead of an increasing one as in the CC reference (Figure 2). In particular, the twisted CT state is considerably more stable than the untwisted LE state, at odds with the CCSD(T) reference calculations. In contrast, BSE/evGW using as input the Kohn–Sham (KS) eigenstates generated from BLYP does follow a qualitatively correct behavior, *i.e.*, BSE/evGW significantly improves the PES of both states as compared to TD-BLYP. It is interesting to note that the improvements appear not only for the CT state but also for the LE one. Indeed, the excited state energies of both CT and LE states show the same topology as the ones of the reference calculations. Nevertheless, the crossing between both states occurs between 40° and 50°, similarly to CC2, rather than exactly at 50° as predicted by both CCSD and CCSD(T)(a)*. We underline that BSE/evGW/BLYP also provides quantitatively more accurate transition energies than CCSD with smaller Mean Absolute Error (MAE) when using the CCSD(T)(a)* values as reference (see Table S3 in the SM).

Starting the BSE/evGW calculations with Kohn-Sham eigenstates generated with the BLYP functional, that does not contain any exact exchange, was a stringent test to explore the ability of the BSE scheme to properly construct optical excitations from Kohn-Sham eigenstates corrected by the evGW approach. We further confirm the ability of BSE/evGW to wash out the starting point dependency, that plagues TD-DFT, by using different KS input eigenstates : those of global hybrid functionals with 20% and 50% of exact exchange (B3LYP and BHLYP), as well as those of the range-separated CAM-B3LYP functional. The results of BSE/evGW and TD-DFT calculations on the interpolated geometries are presented in Figure 3. Additional examples with other functionals used as a starting point for BSE/evGW calculations and the corresponding TD-DFT data can be found in the SM.

Clearly, at the TD-DFT level, the dependence on the functional is dramatic for the CT state, as expected, but also for the LE excitation that acquires a significant CT character with increasing twist angle. In contrast, BSE/evGW values are very close to each other for both states irrespective

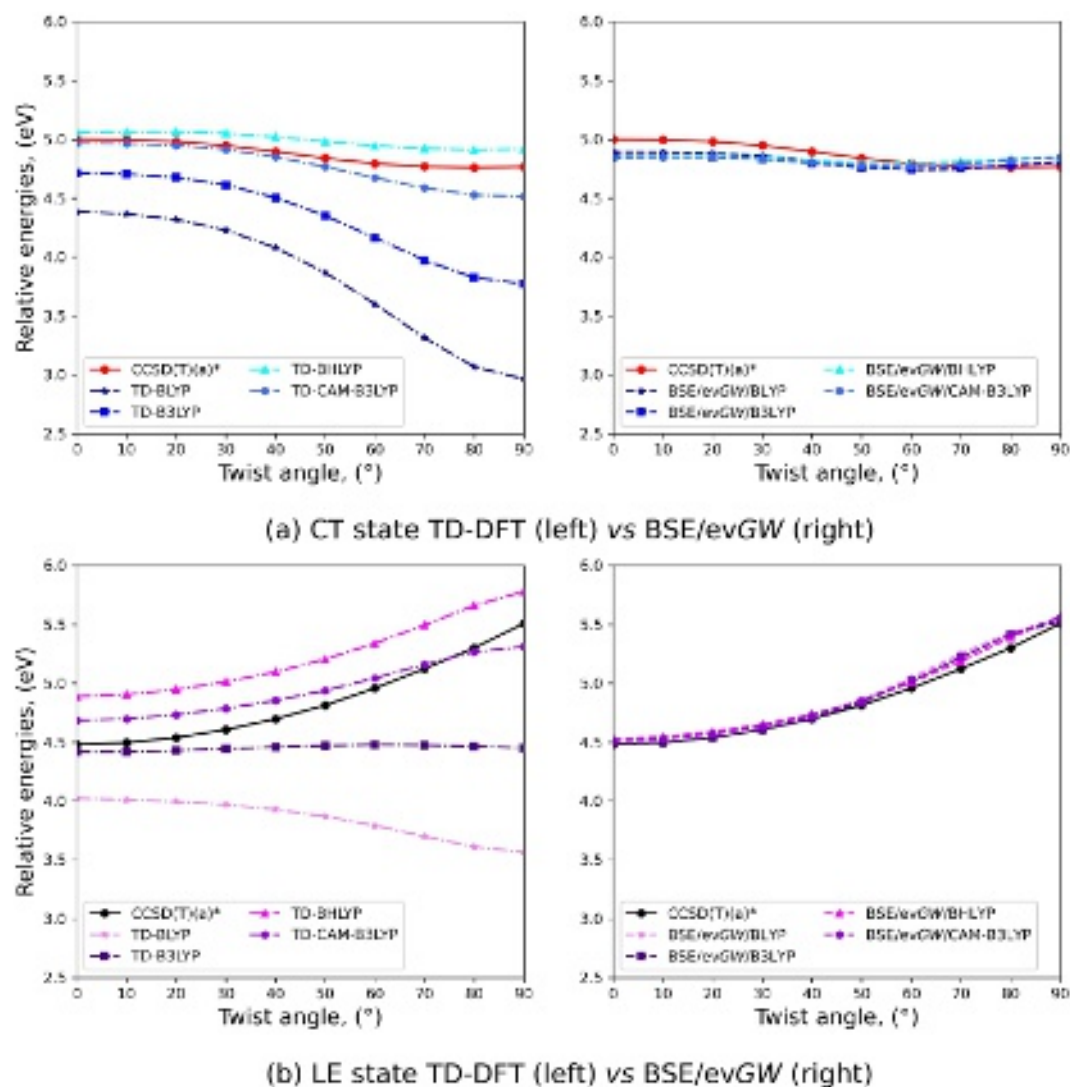


FIG. 3. Comparison of the PES for the CT (a) and LE (b) states of DMABN obtained on CCSD(T)-interpolated geometries with TD-DFT and BSE/evGW methods using the BLYP, B3LYP, BHLYP, and CAM-B3LYP functionals. Relative energies use the GS energy of the untwisted molecule as reference. GS calculations carried out with the corresponding DFT functional for the BSE/evGW calculations.

of the KS eigenstates: the impact of the starting point is very limited. Even though one can notice slight differences between PBE (or PBE0) and BLYP (or B3LYP) BSE results, the variations of the relative energies between these two groups of functionals do not exceed 0.1 eV. Additionally, the MAE values as compared to CCSD(T)(a)* are below 0.1 eV for all BSE/evGW methods irrespective of the starting point (see Tables S3-S8). Thus, we can conclude that there is a very small dependency of the BSE PES on the selected XCF. While this was known for the transition energies,^{51,56} it is the first demonstration that it also holds for complex PES topologies associated

with excitations showing pure or hybrid CT character.

Interestingly, even though TD-CAM-B3LYP greatly improves the quality of the excited state surfaces as compared to TD-BLYP, BSE/evGW/CAM-B3LYP provides excited state energies of twisted structures which are both close to their BSE/evGW/BLYP counterpart and in agreement with reference values (see Table S6). Such a lack of dependency on the input Kohn-Sham eigenstates, together with the ability to describe accurately both localized, CT and hybrid states, is a significant advantage of the BSE/evGW scheme.

We also calculated CT and LE state energies using BSE/evGW and TD-DFT methods on optimized structures (Figure S4). In the same way as for interpolated geometries, BSE/evGW yields accurate PES for both states. As in CC, the relaxation affects the position of the crossing between CT and LE states - it occurs at 50° twist angle. Additionally, BSE/evGW captures the shallow minima on the LE PES independently of the functional selected as a starting point.

This work stands as a clear indication (Figure 3) that the development of BSE/evGW ES analytic gradients, would be welcome as they are based on more accurate energies, at least for CT ESs, but also possibly for LE ones.

C. Solvatochromic effects

In this Section we present the PESs of DMABN modelled in hexane and acetonitrile. We discuss here only the results obtained from the vertical transition calculations on the ground state Hexane-PTED-CCSD and MeCN-PTED-CCSD optimized geometries. Nevertheless, we also provide the SS-PTED-EOM-CCSD optimized PES of both the LE and CT states in both solvents in the SM (Figure S5). Let us start with a comparison between PTED-EOM-CCSD (LR and SS formalisms), PCM-BSE/evGW/B3LYP, cLR²-PCM-TD-B3LYP, and cLR²-PCM-TD-CAM-B3LYP (see Figure 4). One first observes that, at the EOM-CCSD level, LR-PTED is not able to properly describe the decrease of the ES energies of the CT state during the twist, and thus the SS formalism should be used in that case. This was expected as in the CT state at 90° the transition dipole moment is essentially null (hence the LR corrections are negligible) whereas the electron density reorganization is large. As a result, only the SS approach leads to a twisted CT state slightly lower in energy than the untwisted LE state, consistently with the appearance of the red-shifted TICT fluorescence band in the presence of polar solvents. However, the SS formalism also leads to nonphysical lowering of CT state energy in hexane, such behaviour of SS methods was observed

in previous works as well.^{25,28} In the following, EOM-CCSD simply refers to SS-PTED-EOM-CCSD.

The same trends can be seen when comparing the LR, cLR, a SS-like method, and cLR², that accounts for both LR and SS, in TD-DFT (see Figure S6 in the SM). Similarly to the gas phase, the evolution of the excited state surfaces for both states is greatly improved using the PCM-BSE/evGW/B3LYP or cLR²-PCM-TD-CAM-B3LYP methods as compared to the cLR²-PCM-TD-B3LYP approach that clearly fails to deliver a sound result. Indeed in TD-DFT, the selection of the XCF and solvent model are known to be dependent: both have to be adequate to obtain an accurate description.¹⁰² In contrast, we recall that the PCM-BSE/evGW scheme hardly depends on the input Kohn-Sham eigenstates and consistently includes both LR and SS effects.⁹⁵

Looking at the Figure 4 it is seen that the cLR²-PCM-TD-CAM-B3LYP energies are closer to the EOM-CCSD ones, while the PCM-BSE/evGW values are a bit lower. Since EOM-CCSD tends to overestimate the transition energies (see the discussions above) it is quite reasonable to state that PCM-BSE/evGW provides accurate results in the condensed phase for DMABN. Further, the CT state is too low in energy as compared to the LE one at the cLR²-PCM-TD-CAM-B3LYP level in both solvents, leading to an overstabilized twisted CT state, especially in hexane. We stress that this is not a solvent effect, since TD-CAM-B3LYP overstabilizes the CT energies at large twist angle as compared to BSE and CC already in the gas phase. In contrast, PCM-BSE/evGW predicts twisted CT above its untwisted LE counterpart in both solvents, i.e., the CT state is not stabilized enough in acetonitrile. Such behaviour may be associated with the slight increase of the CT energy beyond 70° already observed in the gas phase.

Additionally, in Figure S11 and Tables S10–S13 in the SM, we provide the vertical excitation energies as well as differences between the energies determined for the 0° and 90° structures ($\Delta E^{0^\circ-90^\circ}$). We highlight here that although the PCM-BSE/evGW/B3LYP method is not perfectly agreeing with some of the EOM-CCSD trends (especially for relative energies of the CT state, Figure 4) it qualitatively reproduces the energetic changes upon twisting for vertical transition energies. The graphs in Figure S11 and $\Delta E^{0^\circ-90^\circ}$ values in Tables S12-S13 indeed show that PCM-BSE/evGW/B3LYP vertical absorption energies are closer to the SS-PTED-EOM-CCSD than to the LR-PTED-EOM-CCSD ones. While PCM-BSE/evGW/B3LYP transition energies are in good agreement with the reference CC values, the corresponding TD-DFT level predicts too low transition energies for both states, especially at large twist angles.

Moreover, BSE/evGW predicts a crossing point between the CT and LE states (around 45°

This is the author's peer reviewed, accepted manuscript. However, the online version of record will be different from this version once it has been copyedited and typeset.
PLEASE CITE THIS ARTICLE AS DOI:10.1063/5.0121121

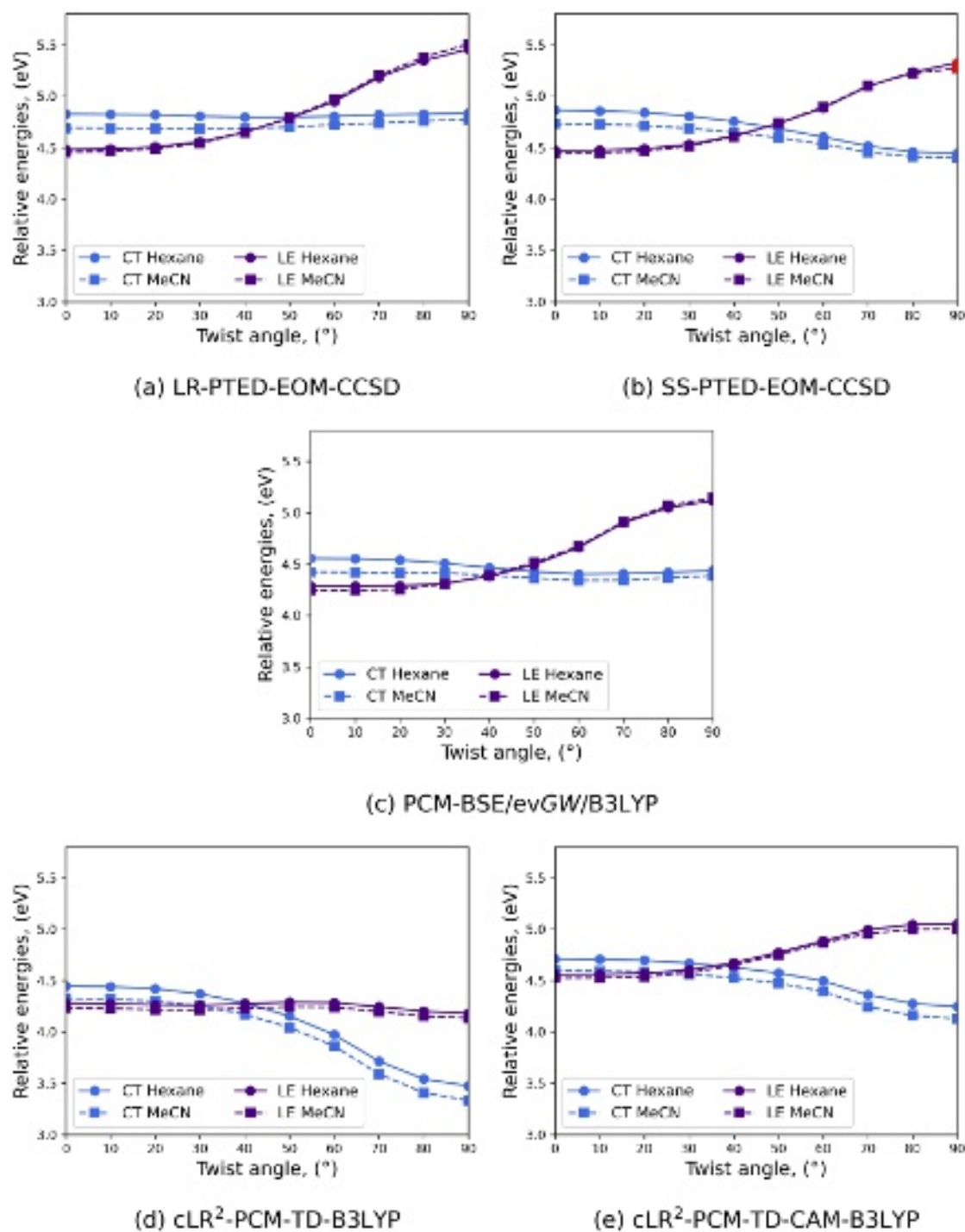


FIG. 4. Hexane (solid line) and acetonitrile (dotted line) PESs for the CT and LE states of DMABN obtained on PTED-CCSD-optimized geometries in the corresponding solvent using (a) LR-PTED-EOM-CCSD, (b) SS-PTED-EOM-CCSD, (c) PCM-BSE/evGW/B3LYP, (d) cLR²-PCM-TD-B3LYP, and (e) cLR²-PCM-TD-CAM-B3LYP methods. Relative energies use the solvated GS energy of the untwisted molecule as reference (the PCM-B3LYP GS energy was selected for the BSE/evGW/B3LYP calculations). Points marked with red in panel (b) were obtained by extrapolation, see the SM for details.

in hexane and 40° in acetonitrile) closer to the EOM-CCSD value (50° and 40°, respectively) than TD-CAM-B3LYP (40° and 30°, respectively). The gap between the LE and CT states in the 0°–40° region is smaller in acetonitrile than hexane according to EOM-CCSD. While this trend is well reproduced by BSE/evGW, TD-CAM-B3LYP predicts the CT and LE energies to be too close from one another in acetonitrile.

An alternative strategy in evaluating the accuracy of the theoretically predicted solvated ES energies is to compare the solvatochromic shifts, *i.e.*, the difference between solvated (ΔE_{solv}) and gas phase vertical absorption energies (ΔE_{gas}). Theoretically predicted solvatochromic shifts are presented in Figures S8 (hexane) and S9 (acetonitrile) in the SM, whereas a summary of the evolution of the solvatochromic shifts between 0° and 90° is given in Table I.

TABLE I. Solvatochromic shifts (eV) evolution from the 0° to the 90° geometries (solvated geometries) as obtained with the PCM solvation model in hexane and acetonitrile. The total change of the shift with twist angle is indicated above the corresponding arrow. The data correspond to Fig. S7 (hexane) and S8 (acetonitrile) in the SM.

	CT		LE	
	Hexane			
LR-PTED-EOM-CCSD	-0.19	$\xrightarrow{+0.11}$	-0.08	-0.03 $\xrightarrow{+0.02}$ -0.01
SS-PTED-EOM-CCSD	-0.15	$\xrightarrow{-0.32}$	-0.47	-0.04 $\xrightarrow{-0.10}$ -0.14 ^a
LR-PCM-TD-B3LYP	-0.16	$\xrightarrow{+0.06}$	-0.10	-0.04 $\xrightarrow{-0.01}$ -0.05
cLR ² -PCM-TD-B3LYP	-0.18	$\xrightarrow{-0.13}$	-0.31	-0.07 $\xrightarrow{-0.19}$ -0.26
LR-PCM-TD-CAM-B3LYP	-0.15	$\xrightarrow{+0.06}$	-0.09	-0.03 $\xrightarrow{-0.02}$ -0.05
cLR ² -PCM-TD-CAM-B3LYP	-0.17	$\xrightarrow{-0.11}$	-0.28	-0.05 $\xrightarrow{-0.20}$ -0.25
PCM-BSE/evGW/B3LYP	-0.20	$\xrightarrow{-0.16}$	-0.36	-0.11 $\xrightarrow{-0.26}$ -0.37
	Acetonitrile			
LR-PTED-EOM-CCSD	-0.31	$\xrightarrow{+0.12}$	-0.19	-0.04 $\xrightarrow{+0.03}$ -0.01
SS-PTED-EOM-CCSD	-0.27	$\xrightarrow{-0.29}$	-0.56	-0.06 $\xrightarrow{-0.18}$ -0.24 ^a
LR-PCM-TD-B3LYP	-0.27	$\xrightarrow{+0.03}$	-0.24	-0.08 $\xrightarrow{-0.04}$ -0.12
cLR ² -PCM-TD-B3LYP	-0.30	$\xrightarrow{-0.21}$	-0.51	-0.11 $\xrightarrow{-0.26}$ -0.37
LR-PCM-TD-CAM-B3LYP	-0.24	$\xrightarrow{+0.03}$	-0.21	-0.06 $\xrightarrow{-0.05}$ -0.11
cLR ² -PCM-TD-CAM-B3LYP	-0.27	$\xrightarrow{-0.18}$	-0.45	-0.08 $\xrightarrow{-0.28}$ -0.36
PCM-BSE/evGW/B3LYP	-0.32	$\xrightarrow{-0.16}$	-0.48	-0.14 $\xrightarrow{-0.28}$ -0.42

^a These solvatochromic shifts were calculated from the solvated vertical absorption energies that were obtained using the extrapolated total ES energies. See the SM for more details.




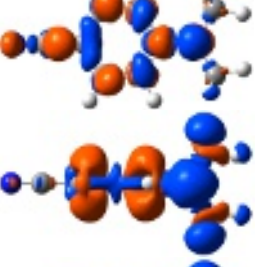

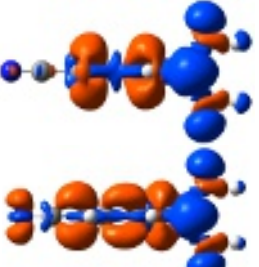
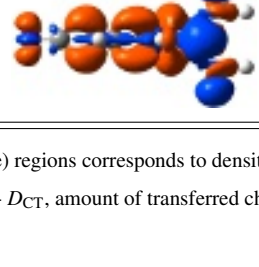
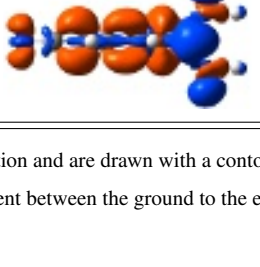
Going from the apolar to the polar solvent leads to an increase of the solvatochromic shifts yet does not strongly influence their evolution along the twist coordinate.¹⁰³ Nevertheless, the

discussion of the trends that is provided below holds for both solvents. Clearly, the shifts are highly dependent on the selected formalism (LR or SS) for both states. Further, the evolutions of the shift with twist angle clearly differ between LR and SS, the LR bathochromic shifts decreasing with twist angle for the CT, in contrast with the SS shift. An analysis of the solvatochromic shifts as a function of the twist angle (Figs. S8 and S9) shows that below 40° both contributions are close, whereas at larger twist angles, the SS corrections significantly increase in particular, but not exclusively, for the CT state. Moreover, as can be seen from Table I at 0° all the methods provide rather similar shifts for both ES states, while at 90° larger differences arise between the different levels of theory and solvation schemes. This is because the LE and CT states acquire a more mixed character along the twisting coordinate with LE gaining some CT character at large twist angle (and CT a partial local character at small twist). To support this statement we calculated the CT parameters (D_{CT} , q_{CT} and μ_{CT}), see Table II. These data show that changing the twisting angle from 0° to 90° leads to significant increase in CT parameters, especially for LE state, indicating that both states at 90° have significant charge transfer character. Additionally, a considerable increase in D_{CT} and μ_{CT} for CT states and LE at 90° can be observed in acetonitrile compared to hexane. As BSE/evGW accounts for both LR and SS effects simultaneously, it works well for states with mixed character. As a result, we can see that both the PCM-BSE/evGW method as well as cLR²-TD-CAM-B3LYP are closer to LR-PTED-EOM-CCSD values in the small twist region and mimic SS-PTED-EOM-CCSD ones in the large twist region which is a physically reasonable trend.

In order to further compare the LR and SS contributions we also computed the difference between the solvated vertical absorption energies (ΔE_{solv}) and the transition energies obtained freezing the ground state polarization at the BSE/evGW and TD-DFT levels of theory in hexane (see Figure S10 in the SM) and in acetonitrile (see Figure 5). ΔE_{ω_0} includes the solvent contribution for the molecular orbitals but does not contain "ES solvation terms". This splitting of the different contribution supports the above mentioned conclusions regarding the importance of the SS correction at the large twist angle as well as the need to include both LR and SS in order to properly describe the ESs of DMABN. Moreover, the graphs on Figure 5 clearly show that the PCM-BSE/evGW and cLR²-TD-DFT models are following the same trends in terms of ES contributions.

To sum up the solvent results for DMABN, we can state that PCM-BSE/evGW provides more accurate vertical transition energies than TD-DFT in the case of ESs having a mixed LE/CT character. However, the PCM-BSE/evGW total ES energies (relative to the untwisted GS reference)

TABLE II. Density difference plot^a and CT parameters^b for 0° and 90° geometries of DMABN determined using the LR-PCM-TD-CAM-B3LYP/cc-pVTZ level of theory.

(°)	State	Hexane			Acetonitrile				
		Density difference plot	D_{CT} [Å]	q_{CT} [e]	μ_{CT} [D]	Density difference plot	D_{CT} [Å]	q_{CT} [e]	μ_{CT} [D]
0	LE		0.855	0.505	0.432		0.980	0.559	0.548
	CT		1.744	0.445	0.776		2.091	0.509	1.064
90	LE		1.899	1.104	2.096		2.149	1.116	2.398
	CT		2.190	1.033	2.256		2.509	1.054	2.644

^a The red (blue) regions corresponds to density increase (decrease) upon absorption and are drawn with a contour threshold of 0.002 au.

^b CT distance - D_{CT} , amount of transferred charge - q_{CT} , change in dipole moment between the ground to the excited states - μ_{CT} .

appear not stabilized enough at high twist angles in the polar medium.

IV. COMPARISON WITH EXPERIMENTAL RESULTS

Dual fluorescence of the DMABN was extensively studied experimentally.^{1,6,7,9} Thus, it looks natural to compare the theoretical estimates to experimental observations. To this end, we used optimized minima for the GS, LE and CT states in the gas phase and acetonitrile. In solution we consider absorption only since there is to-date no BSE/evGW approach allowing to polarize the solvent cavity using the excited-state density (as it should for emission). The calculated and experimental absorption and emission energies are listed in Table III. First, one can notice that theoretical values overestimates their experimental counterparts, which was expected as all vibronic effects are neglected, and such comparison therefore remains qualitative.^{41,104} This is why we compare trends rather than absolute values. The data in the Table III show that in the gas phase BSE/evGW delivers a more accurate CT-LE absorption gap (0.33 eV vs 0.44 eV experimentally) than TD-DFT

This is the author's peer reviewed, accepted manuscript. However, the online version of record will be different from this version once it has been copyedited and typeset. PLEASE CITE THIS ARTICLE AS DOI:10.1063/5.0121121

This is the author's peer reviewed, accepted manuscript. However, the online version of record will be different from this version once it has been copyedited and typeset.
PLEASE CITE THIS ARTICLE AS DOI:10.1063/5.0121121

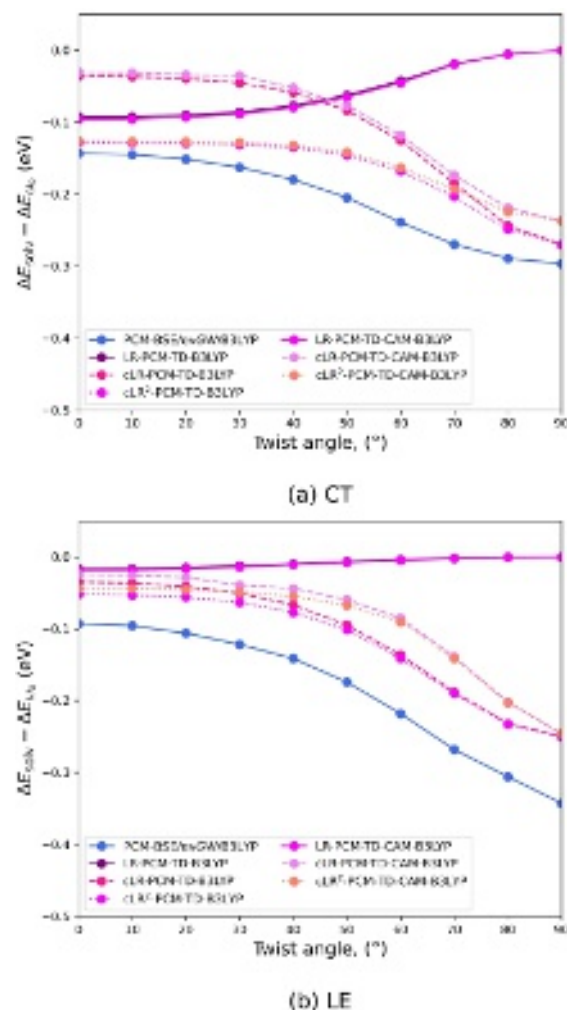


FIG. 5. Acetonitrile solvent shifts ($\Delta E_{\text{solv}} - \Delta E_{\text{vib}}$) between the solvated vertical absorption energies (ΔE_{solv}) and the ground state frozen polarization energy (ΔE_{vib}) for the CT (a) and LE (b) of DMABN computed on MeCN-PTED-CCSD-optimized geometries with PCM-BSE/evGW/B3LYP and TD-DFT (LR, cLR, and cLR²) combined with the B3LYP and CAM-B3LYP functionals.

(0.23 eV with both functionals). More importantly, in acetonitrile, BSE/evGW underestimates the experimental CT-LE by 0.13 eV, while the most refined TD-DFT scheme (cLR²-PCM-TD-CAM-B3LYP) is off the experimental value by 0.32 eV. In addition, solvatochromic shifts from the gas phase to acetonitrile are more accurately predicted by BSE/evGW than both TD-CAM-B3LYP and EOM-CCSD. In gas-phase, the experimental Stokes shift attains 0.45 eV for LE and 1.02 eV for CT, but the latter value is extrapolated. All approaches deliver quite reasonable estimates for the former: 0.56 eV (BSE/evGW), 0.52 eV (EOM-CCSD), and 0.53 eV (TD-CAM-B3LYP), but overshoots the CT Stokes shift (1.88 eV for BSE/evGW, 1.94 eV for EOM-CCSD, and 2.13 eV for TD-CAM-B3LYP), part of the error possibly coming from the experimental uncertainties.

TABLE III. Comparison between experimental²³ absorption ($\Delta E_{\text{abs}}^{\text{exp}}$) and emission ($\Delta E_{\text{em}}^{\text{exp}}$) maxima, calculated vertical absorption ($\Delta E_{\text{abs}}^{\text{calc}}$) and emission ($\Delta E_{\text{em}}^{\text{calc}}$) energies. The cc-pVTZ atomic basis set was employed for computing transition energies.

Method	Calculated				Experimental			
	$\Delta E_{\text{abs}}^{\text{calc}}$		$\Delta E_{\text{em}}^{\text{calc}}$		$\Delta E_{\text{abs}}^{\text{exp}}$		$\Delta E_{\text{em}}^{\text{exp}}$	
	LE	CT	LE	CT	LE	CT	LE	CT
Gas phase								
EOM-CCSD	4.58	5.07	4.06	3.13				
TD-B3LYP	4.41	4.64	3.87	2.20	4.13	4.57	3.68	3.55 ^a
TD-CAM-B3LYP	4.68	4.91	4.15	2.78				
BSE/evGW/B3LYP	4.48	4.81	3.92	2.93				
Acetonitrile								
LR-EOM-CCSD	4.52	4.75	-	-				
SS-EOM-CCSD	4.51	4.86	-	-				
cLR ² -PCM-TD-B3LYP	4.29	4.34	-	-	3.86	4.21	3.44	2.52
cLR ² -PCM-TD-CAM-B3LYP	4.59	4.62	-	-				
PCM-BSE/evGW/B3LYP	4.34	4.56	-	-				

^a The experimental CT emission energy in the gas phase is an extrapolated value.

V. CONCLUSIONS

We have shown that BSE/evGW is able to accurately reproduce the evolution of the excited state PESs of the two key ESs of DMABN upon twisting, a known challenging case for TD-DFT. We provided accurate benchmark surfaces calculated at CCSD(T)(a)*/cc-pVTZ and CCSD/cc-pVTZ levels of theory in the gas phase and PTED-EOM-CCSD/cc-pVTZ (LR and SS) in both hexane and acetonitrile. The excited state surfaces obtained with the high-level theories allowed us to access the accuracy of the BSE/evGW formalisms for modeling the ES PESs of DMABN in both gas and solvated phases.

The results from the gas phase calculations indicate that BSE/evGW is able to reproduce the correct evolution of the ES PESs upon twisting of DMABN. Moreover, BSE/evGW shows negligible starting point (various DFT functionals) dependency, and the computed vertical excited state energies are more accurate than TD-DFT's when CCSD(T)(a)* values are taken as a reference. Modeling the PESs in solution is more complicated than in the gas phase due not only to the additional computational costs but also to the existence of various approximations to model solvatochromisms. Nevertheless, we have shown that BSE/evGW combined with the PCM formalism predicts a globally accurate topology for the LE and CT PESs of DMABN in solution as well,

likely because both LR and SS effects are captured, which is important for states with a mixed LE/CT character.

This work stands as a positive hint that BSE/evGW should be able to deliver accurate shapes for the excited state PES of a diversity of ESs. It is therefore an additional motivation to develop analytic BSE/evGW gradients, both in the gas phase and in the presence of a solvent or a reactive medium in general.

ACKNOWLEDGMENTS

The authors are grateful to Prof. Marco Caricato for his kind help with PTED-CCSD calculations. This work received support from the French Agence Nationale de la Recherche (ANR) under contract ANR-20-CE29-0005 (BSE-Forces). This work used computational resources generously provided by the CCIPL computational center installed in Nantes and the national HPC facilities under contract GENCI-TGCC A0110910016.

SUPPLEMENTARY MATERIAL

See the Supplementary Material for additional data (potential energy surfaces, additional functional test, and solvatochromic effects), discussion of the energetic differences between the twisted and untwisted structure, extrapolation procedure, and Cartesian coordinates.

DATA AVAILABILITY

See the Supplementary Material - further data available on request to the authors.

AUTHOR DECLARATIONS

Conflict of Interest

The authors have no conflicts to disclose.

Author Contributions

Iryna Knysh: Calculations and data curation (lead); Formal analysis (equal); Validation (equal); Writing – original draft (lead). **Ivan Duchemin:** Calculations and data curation (equal); Software (lead); Validation (equal). **Xavier Blase:** Design and conceptualization (equal); Investigation (equal); Validation (equal); Writing – review & editing (equal). **Denis Jacquemin:** Design and conceptualization (equal); Investigation (equal); Supervision (lead); Validation (equal); Writing – review & editing (equal).

REFERENCES

- ¹E. Lippert, W. Ludar, and H. Boss, *Advances in Molecular Spectroscopy* (Pergamon Press, Oxford, 1962).
- ²C. Wang, W. Chi, Q. Qiao, D. Tan, Z. Xu, and X. Liu, *Chem. Soc. Rev.* **50**, 12656 (2021).
- ³U. Leinhos, W. Kuehnle, and K. A. Zachariasse, *J. Phys. Chem.* **95**, 2013 (1991).
- ⁴K. Rotkiewicz, K. Grellmann, and Z. Grabowski, *Chem. Phys. Lett.* **19**, 315 (1973).
- ⁵W. Schuddeboom, S. A. Jonker, J. M. Warman, U. Leinhos, W. Kuehnle, and K. A. Zachariasse, *J. Phys. Chem.* **96**, 10809 (1992).
- ⁶K. A. Zachariasse, T. von der Haar, A. Hebecker, U. Leinhos, and W. Kuehnle, *Pure Appl. Chem.* **65**, 1745 (1993).
- ⁷S. I. Druzhinin, N. P. Ernsting, S. A. Kovalenko, L. P. Lustres, T. A. Senyushkina, and K. A. Zachariasse, *J. Phys. Chem. A* **110**, 2955 (2006).
- ⁸A. L. Sobolewski and W. Domcke, *Chem. Phys. Lett.* **259**, 119 (1996).
- ⁹Z. R. Grabowski, K. Rotkiewicz, and W. Rettig, *Chem. Rev.* **103**, 3899 (2003).
- ¹⁰A. L. Sobolewski, W. Sudholt, and W. Domcke, *J. Phys. Chem. A* **102**, 2716 (1998).
- ¹¹O. Christiansen, H. Koch, and P. Jørgensen, *Chem. Phys. Lett.* **243**, 409 (1995).
- ¹²C. Hättig and F. Weigend, *J. Chem. Phys.* **113**, 5154 (2000).
- ¹³C. Hättig, *J. Chem. Phys.* **118**, 7751 (2003).
- ¹⁴A. Köhn and C. Hättig, *J. Chem. Phys.* **119**, 5021 (2003).
- ¹⁵A. Köhn and C. Hättig, *J. Am. Chem. Soc.* **126**, 7399 (2004).
- ¹⁶J. Tomasi, B. Mennucci, and R. Cammi, *Chem. Rev.* **105**, 2999 (2005).
- ¹⁷C. A. Guido and S. Caprasecca, *Int. J. Quantum Chem.* **119**, e25711 (2019).

This is the author's peer reviewed, accepted manuscript. However, the online version of record will be different from this version once it has been copyedited and typeset.
PLEASE CITE THIS ARTICLE AS DOI:10.1063/5.0121121

- ¹⁸B. Lunkenheimer and A. Köhn, *J. Chem. Theory Comput.* **9**, 977 (2013).
- ¹⁹M. Caricato, *J. Chem. Phys.* **139**, 044116 (2013).
- ²⁰I. Duchemin, C. A. Guido, D. Jacquemin, and X. Blase, *Chem. Sci.* **9**, 4430 (2018).
- ²¹C. A. Guido, A. Chrayteh, G. Scalmani, B. Mennucci, and D. Jacquemin, *J. Chem. Theory Comput.* **17**, 5155 (2021).
- ²²B. Mennucci, A. Toniolo, and J. Tomasi, *J. Am. Chem. Soc.* **122**, 10621 (2000).
- ²³I. Georgieva, A. J. A. Aquino, F. Plasser, N. Trendafilova, A. Köhn, and H. Lischka, *J. Phys. Chem. A* **119**, 6232 (2015).
- ²⁴A. Klamt and G. Schüürmann, *J. Chem. Soc., Perkin Trans. 2*, 799 (1993).
- ²⁵J.-M. Mewes, J. M. Herbert, and A. Dreuw, *Phys. Chem. Chem. Phys.* **19**, 1644 (2017).
- ²⁶M. Caricato, *J. Chem. Phys.* **148**, 134113 (2018).
- ²⁷M. Caricato, *WIREs Comput. Mol. Sci.* **10**, e1463 (2020).
- ²⁸M. Caricato, *ChemPhotoChem* **3**, 747 (2019).
- ²⁹M. Caricato, *J. Chem. Theory Comput.* **8**, 4494 (2012).
- ³⁰M. Caricato, *J. Chem. Theory Comput.* **8**, 5081 (2012).
- ³¹E. Runge and E. K. U. Gross, *Phys. Rev. Lett.* **52**, 997 (1984).
- ³²M. E. Casida, “Time-dependent density functional response theory for molecules,” in *Recent Advances in Density Functional Methods*, Vol. 1, edited by D. P. Chong (World Scientific: Singapore, 1995) pp. 155–192.
- ³³A. B. J. Parusel, G. Köhler, and S. Grimme, *J. Phys. Chem. A* **102**, 6297 (1998).
- ³⁴C. Jamorski Jödicke and H. P. Lüthi, *J. Am. Chem. Soc.* **125**, 252 (2003).
- ³⁵D. Rappoport and F. Furche, *J. Am. Chem. Soc.* **126**, 1277 (2004).
- ³⁶D. J. Tozer, *J. Chem. Phys.* **119**, 12697 (2003).
- ³⁷A. Dreuw and M. Head-Gordon, *J. Am. Chem. Soc.* **126**, 4007 (2004).
- ³⁸P. Wiggins, J. A. G. Williams, and D. J. Tozer, *J. Chem. Phys.* **131**, 091101 (2009).
- ³⁹M. J. G. Peach, P. Benfield, T. Helgaker, and D. J. Tozer, *J. Chem. Phys.* **128**, 044118 (2008).
- ⁴⁰T. Yanai, D. P. Tew, and N. C. Handy, *Chem. Phys. Lett.* **393**, 51 (2004).
- ⁴¹A. D. Laurent and D. Jacquemin, *Int. J. Quantum Chem.* **113**, 2019 (2013).
- ⁴²E. E. Salpeter and H. A. Bethe, *Phys. Rev.* **84**, 1232 (1951).
- ⁴³W. Hanke and L. J. Sham, *Phys. Rev. Lett.* **43**, 387 (1979).
- ⁴⁴G. Strinati, *Riv. del Nuovo Cim.* **11**, 1 (1988).
- ⁴⁵L. Hedin, *Phys. Rev.* **139**, A796 (1965).

This is the author's peer reviewed, accepted manuscript. However, the online version of record will be different from this version once it has been copyedited and typeset.
PLEASE CITE THIS ARTICLE AS DOI:10.1063/5.0121121

- ⁴⁶I. Duchemin, T. Deutsch, and X. Blase, *Phys. Rev. Lett.* **109**, 167801 (2012).
- ⁴⁷B. Baumeier, D. Andrienko, and M. Rohlfing, *J. Chem. Theory Comput.* **8**, 2790 (2012).
- ⁴⁸I. Duchemin and X. Blase, *Phys. Rev. B* **87**, 245412 (2013).
- ⁴⁹P. Cudazzo, M. Gatti, A. Rubio, and F. Sottile, *Phys. Rev. B* **88**, 195152 (2013).
- ⁵⁰V. Ziaei and T. Bredow, *J. Chem. Phys.* **145**, 174305 (2016).
- ⁵¹D. Jacquemin, I. Duchemin, and X. Blase, *J. Phys. Chem. Lett.* **8**, 1524 (2017).
- ⁵²P. Boulanger, D. Jacquemin, I. Duchemin, and X. Blase, *J. Chem. Theory Comput.* **10**, 1212 (2014).
- ⁵³X. Blase, C. Attaccalite, and V. Olevano, *Phys. Rev. B* **83**, 115103 (2011).
- ⁵⁴F. Kaplan, M. E. Harding, C. Seiler, F. Weigend, F. Evers, and M. J. van Setten, *J. Chem. Theory Comput.* **12**, 2528 (2016).
- ⁵⁵T. Rangel, S. M. Hamed, F. Bruneval, and J. B. Neaton, *J. Chem. Theory Comput.* **12**, 2834 (2016).
- ⁵⁶D. Jacquemin, I. Duchemin, and X. Blase, *J. Chem. Theory Comput.* **11**, 3290 (2015).
- ⁵⁷F. Bruneval, S. M. Hamed, and J. B. Neaton, *J. Chem. Phys.* **142**, 244101 (2015).
- ⁵⁸N. C. Handy and H. F. Schaefer, *The Journal of Chemical Physics* **81**, 5031 (1984).
- ⁵⁹S. Ismail-Beigi and S. G. Louie, *Phys. Rev. Lett.* **90**, 076401 (2003).
- ⁶⁰O. Çaylak and B. Baumeier, *J. Chem. Theory Comput.* **17**, 879 (2021).
- ⁶¹G. D. Purvis and R. J. Bartlett, *J. Chem. Phys.* **76**, 1910 (1982).
- ⁶²J. F. Stanton, J. Gauss, L. Cheng, M. E. Harding, D. A. Matthews, and P. G. Szalay, “CFOUR, Coupled-Cluster techniques for Computational Chemistry, a quantum-chemical program package,” With contributions from A.A. Auer, A. Asthana, R.J. Bartlett, U. Benedikt, C. Berger, D.E. Bernholdt, S. Blaschke, Y. J. Bomble, S. Burger, O. Christiansen, D. Datta, F. Engel, R. Faber, J. Greiner, M. Heckert, O. Heun, M. Hilgenberg, C. Huber, T.-C. Jagau, D. Jonsson, J. Jusélius, T. Kirsch, K. Klein, G.M. Kopper, W.J. Lauderdale, F. Lipparini, J. Liu, T. Metzroth, L.A. Mück, D.P. O’Neill, T. Nottoli, D.R. Price, E. Prochnow, C. Puzzarini, K. Ruud, F. Schiffmann, W. Schwalbach, C. Simmons, S. Stopkowicz, A. Tajti, J. Vázquez, F. Wang, J.D. Watts and the integral packages MOLECULE (J. Almlöf and P.R. Taylor), PROPS (P.R. Taylor), ABACUS (T. Helgaker, H.J. Aa. Jensen, P. Jørgensen, and J. Olsen), and ECP routines by A. V. Mitin and C. van Wüllen. For the current version, see <http://www.cfour.de>.
- ⁶³D. A. Matthews, L. Cheng, M. E. Harding, F. Lipparini, S. Stopkowicz, T.-C. Jagau, P. G. Szalay, J. Gauss, and J. F. Stanton, *J. Chem. Phys.* **152**, 214108 (2020).

This is the author's peer reviewed, accepted manuscript. However, the online version of record will be different from this version once it has been copyedited and typeset.
PLEASE CITE THIS ARTICLE AS DOI:10.1063/5.0121121

- ⁶⁴P.-F. Loos, M. Comin, X. Blase, and D. Jacquemin, *J. Chem. Theory Comput.* **17**, 3666 (2021).
- ⁶⁵M. J. Frisch, G. W. Trucks, H. B. Schlegel, G. E. Scuseria, M. A. Robb, J. R. Cheeseman, G. Scalmani, V. Barone, G. A. Petersson, H. Nakatsuji, X. Li, M. Caricato, A. V. Marenich, J. Bloino, B. G. Janesko, R. Gomperts, B. Mennucci, H. P. Hratchian, J. V. Ortiz, A. F. Izmaylov, J. L. Sonnenberg, D. Williams-Young, F. Ding, F. Lipparini, F. Egidi, J. Goings, B. Peng, A. Petrone, T. Henderson, D. Ranasinghe, V. G. Zakrzewski, J. Gao, N. Rega, G. Zheng, W. Liang, M. Hada, M. Ehara, K. Toyota, R. Fukuda, J. Hasegawa, M. Ishida, T. Nakajima, Y. Honda, O. Kitao, H. Nakai, T. Vreven, K. Throssell, J. A. Montgomery, Jr., J. E. Peralta, F. Ogliaro, M. J. Bearpark, J. J. Heyd, E. N. Brothers, K. N. Kudin, V. N. Staroverov, T. A. Keith, R. Kobayashi, J. Normand, K. Raghavachari, A. P. Rendell, J. C. Burant, S. S. Iyengar, J. Tomasi, M. Cossi, J. M. Millam, M. Klene, C. Adamo, R. Cammi, J. W. Ochterski, R. L. Martin, K. Morokuma, O. Farkas, J. B. Foresman, and D. J. Fox, "Gaussian~16 Revision C.01," (2019), gaussian Inc. Wallingford CT.
- ⁶⁶G. E. Scuseria, A. C. Scheiner, T. J. Lee, J. E. Rice, and H. F. Schaefer, *J. Chem. Phys.* **86**, 2881 (1987).
- ⁶⁷H. Koch, H. J. A. Jensen, P. Jørgensen, and T. Helgaker, *J. Chem. Phys.* **93**, 3345 (1990).
- ⁶⁸J. F. Stanton and R. J. Bartlett, *J. Chem. Phys.* **98**, 7029 (1993).
- ⁶⁹J. F. Stanton, *J. Chem. Phys.* **99**, 8840 (1993).
- ⁷⁰D. A. Matthews and J. F. Stanton, *J. Chem. Phys.* **145**, 124102 (2016).
- ⁷¹O. Christiansen, H. Koch, and P. Jørgensen, *J. Chem. Phys.* **103**, 7429 (1995).
- ⁷²H. Koch, O. Christiansen, P. Jørgensen, and J. Olsen, *Chem. Phys. Lett.* **244**, 75 (1995).
- ⁷³T. H. Dunning, *J. Chem. Phys.* **90**, 1007 (1989).
- ⁷⁴R. A. Kendall, T. H. Dunning, and R. J. Harrison, *J. Chem. Phys.* **96**, 6796 (1992).
- ⁷⁵D. E. Woon and T. H. Dunning, *J. Chem. Phys.* **98**, 1358 (1993).
- ⁷⁶A. K. Wilson, D. E. Woon, K. A. Peterson, and T. H. Dunning, *J. Chem. Phys.* **110**, 7667 (1999).
- ⁷⁷D. E. Woon and T. H. Dunning, *J. Chem. Phys.* **100**, 2975 (1994).
- ⁷⁸A. D. Becke, *Phys. Rev. A* **38**, 3098 (1988).
- ⁷⁹C. Lee, W. Yang, and R. G. Parr, *Phys. Rev. B* **37**, 785 (1988).
- ⁸⁰A. D. Becke, *J. Chem. Phys.* **98**, 1372 (1993).
- ⁸¹J. P. Perdew, K. Burke, and M. Ernzerhof, *Phys. Rev. Lett.* **78**, 1396 (1997).
- ⁸²C. Adamo and V. Barone, *J. Chem. Phys.* **110**, 6158 (1999).
- ⁸³I. Duchemin and X. Blase, *J. Chem. Theory Comput.* **16**, 1742 (2020).

This is the author's peer reviewed, accepted manuscript. However, the online version of record will be different from this version once it has been copyedited and typeset.
PLEASE CITE THIS ARTICLE AS DOI:10.1063/5.0121121

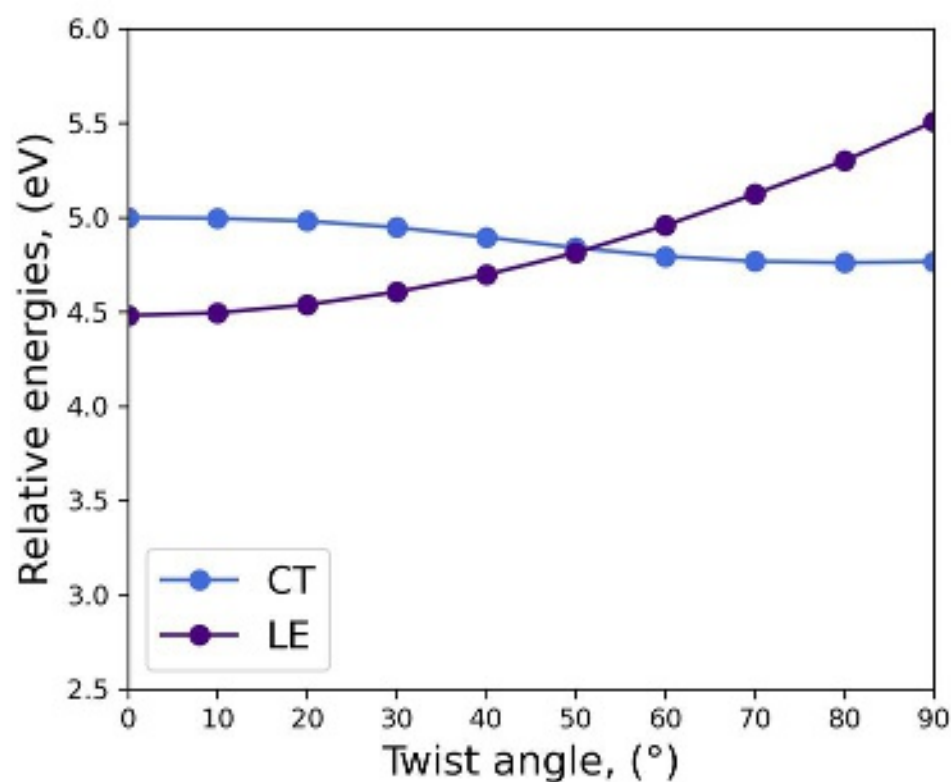
- ⁸⁴X. Blase and C. Attaccalite, Appl. Phys. Lett. **99**, 171909 (2011).
- ⁸⁵X. Ren, P. Rinke, V. Blum, J. Wieferink, A. Tkatchenko, A. Sanfilippo, K. Reuter, and M. Scheffler, New J. Phys. **14**, 053020 (2012).
- ⁸⁶F. Weigend, A. Köhn, and C. Hättig, J. Chem. Phys. **116**, 3175 (2002).
- ⁸⁷F. Neese, WIREs Comput. Mol. Sci. **2**, 73 (2012).
- ⁸⁸F. Neese, F. Wennmohs, U. Becker, and C. Riplinger, J. Chem. Phys. **152**, 224108 (2020).
- ⁸⁹F. Neese, WIREs Comput. Mol. Sci. , e1606 (2022).
- ⁹⁰F. del Valle and J. Tomasi, Chem. Phys. **150**, 139 (1991).
- ⁹¹M. Aguilar, F. del Valle, and J. Tomasi, Chem. Phys. **150**, 151 (1991).
- ⁹²R. Cammi and B. Mennucci, J. Chem. Phys. **110**, 9877 (1999).
- ⁹³M. Cossi and V. Barone, J. Chem. Phys. **115**, 4708 (2001).
- ⁹⁴M. Caricato, B. Mennucci, J. Tomasi, F. Ingrosso, R. Cammi, S. Corni, and G. Scalmani, J. Chem. Phys **124**, 124520 (2006).
- ⁹⁵I. Duchemin, D. Jacquemin, and X. Blase, J. Chem. Phys. **144**, 164106 (2016).
- ⁹⁶A. K. Rappe, C. J. Casewit, K. S. Colwell, W. A. Goddard, and W. M. Skiff, J. Am. Chem. Soc. **114**, 10024 (2002).
- ⁹⁷T. Le Bahers, C. Adamo, and I. Ciofini, J. Chem. Theory Comput. **7**, 2498 (2011).
- ⁹⁸D. Jacquemin, T. L. Bahers, C. Adamo, and I. Ciofini, Phys. Chem. Chem. Phys. **14**, 5383 (2012).
- ⁹⁹M. Schreiber, M. R. Silva-Junior, S. P. A. Sauer, and W. Thiel, J. Chem. Phys. **128**, 134110 (2008).
- ¹⁰⁰D. Kánnár and P. G. Szalay, J. Chem. Theory Comput. **10**, 3757 (2014).
- ¹⁰¹M. Vénil, A. Scemama, M. Caffarel, F. Lipparini, M. Boggio-Pasqua, D. Jacquemin, and P.-F. Loos, WIREs Comput. Mol. Sci. **11**, e1517 (2021).
- ¹⁰²C. A. Guido, D. Jacquemin, C. Adamo, and B. Mennucci, J. Chem. Theory Comput. **11**, 5782 (2015).
- ¹⁰³Nevertheless, few exceptions exist for the cLR²-TD-DFT and PCM-BSE/evGW methods. In the first case as seen from Table I, going from hexane to acetonitrile leads to a bigger increase of solvent shifts difference between 0° and 90° structures (indicated above the arrows in Table I) than for all other methods. In contrast, PCM-BSE/evGW predicts a lowering of the shifts at *ca.* 20° only in the polar medium (see Figure S8).

This is the author's peer reviewed, accepted manuscript. However, the online version of record will be different from this version once it has been copyedited and typeset.
PLEASE CITE THIS ARTICLE AS DOI:10.1063/5.0121121

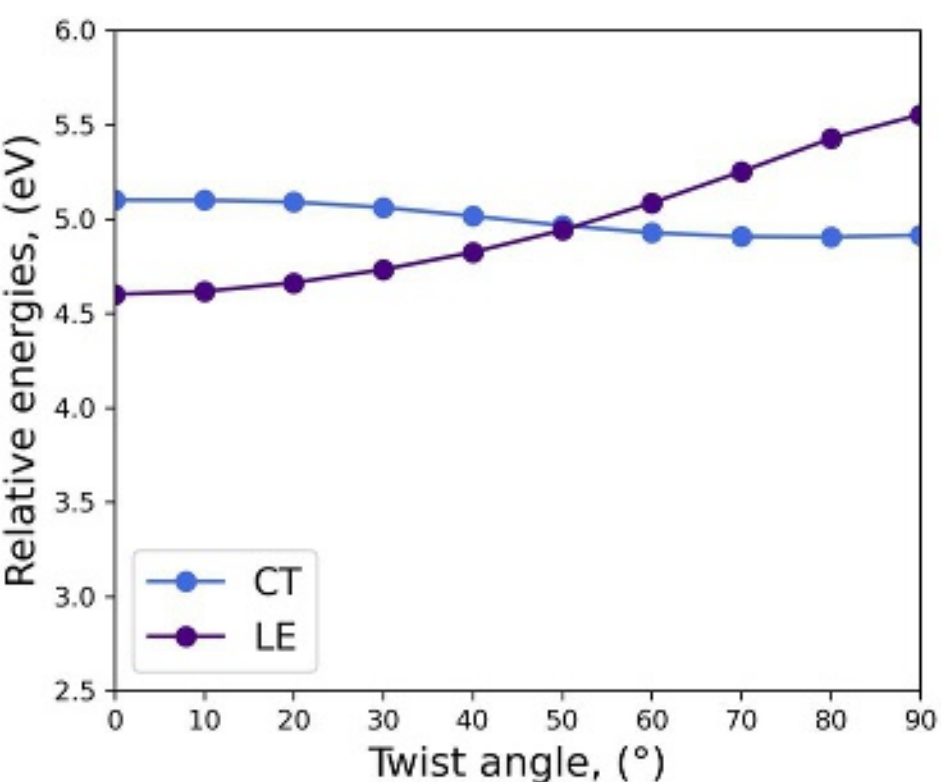
¹⁰⁴D. Jacquemin, E. A. Perpète, I. Ciofini, C. Adamo, R. Valero, Y. Zhao, and D. G. Truhlar, J. Chem. Theory Comput. **6**, 2071 (2010).



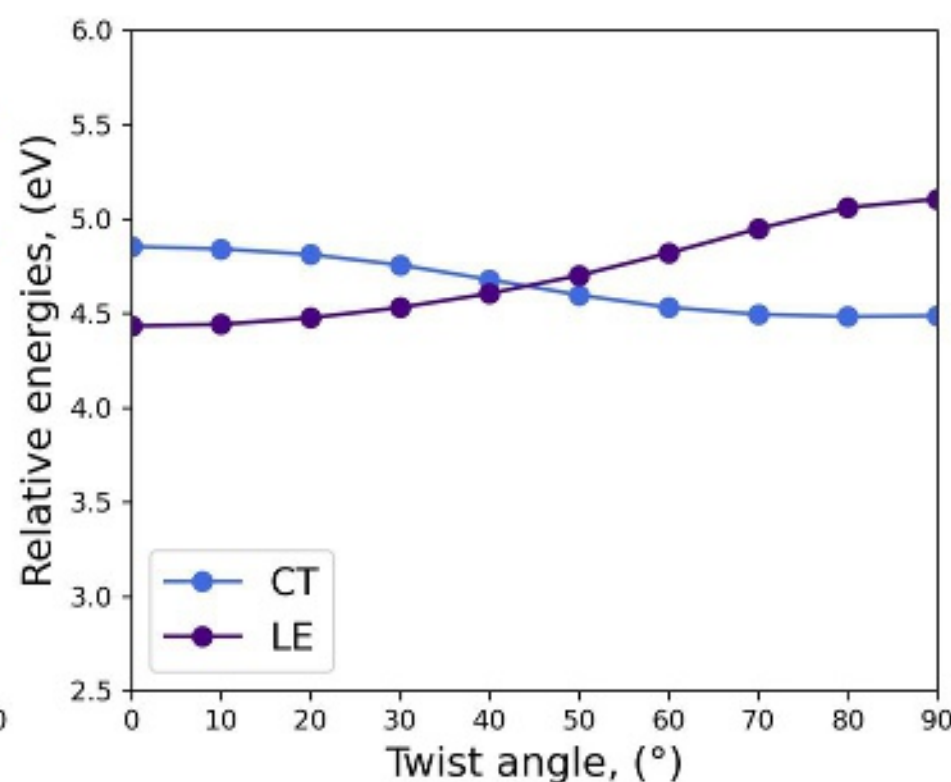
Chem. Phys.
10.1063/5.0121



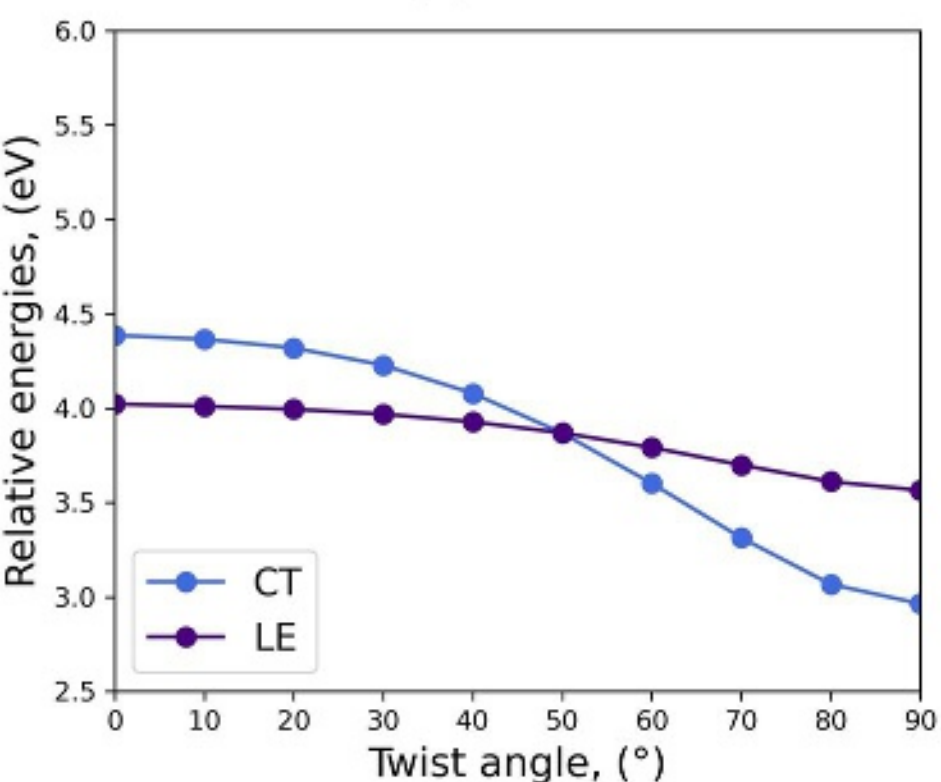
(a) CCSD(T)(a)*



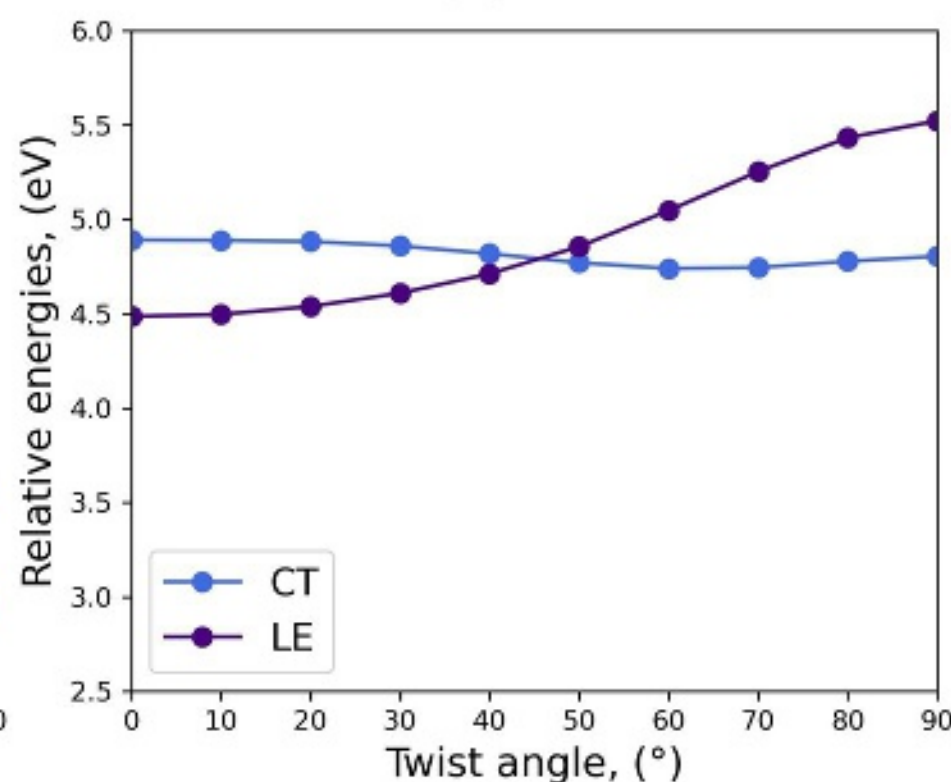
(b) CCSD



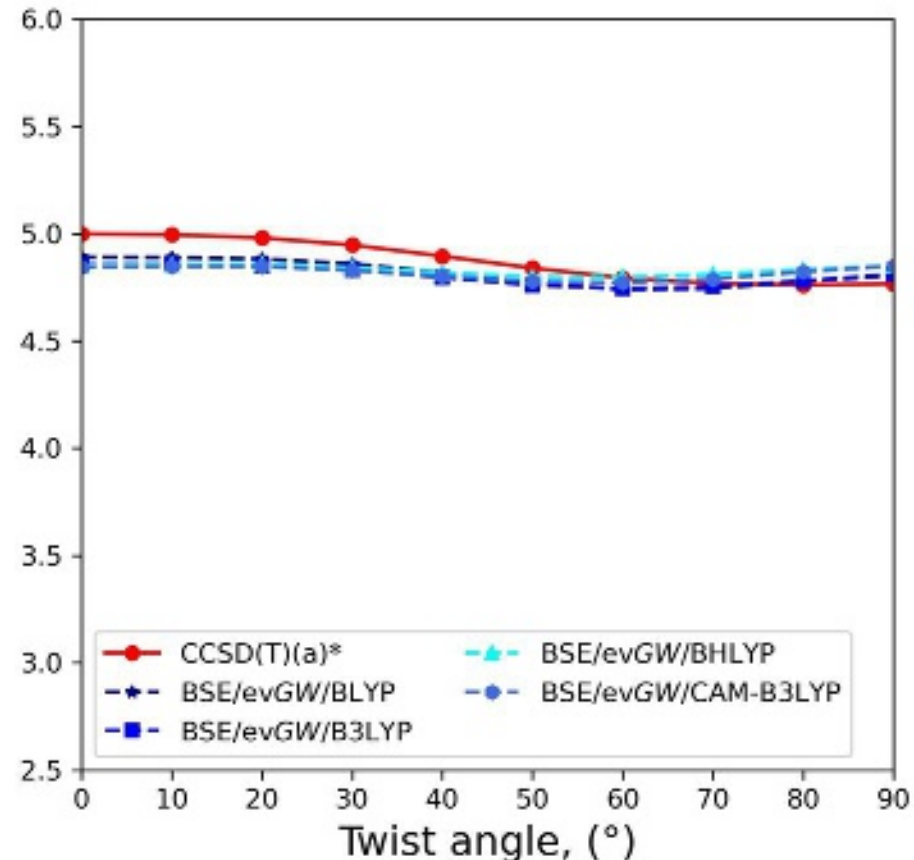
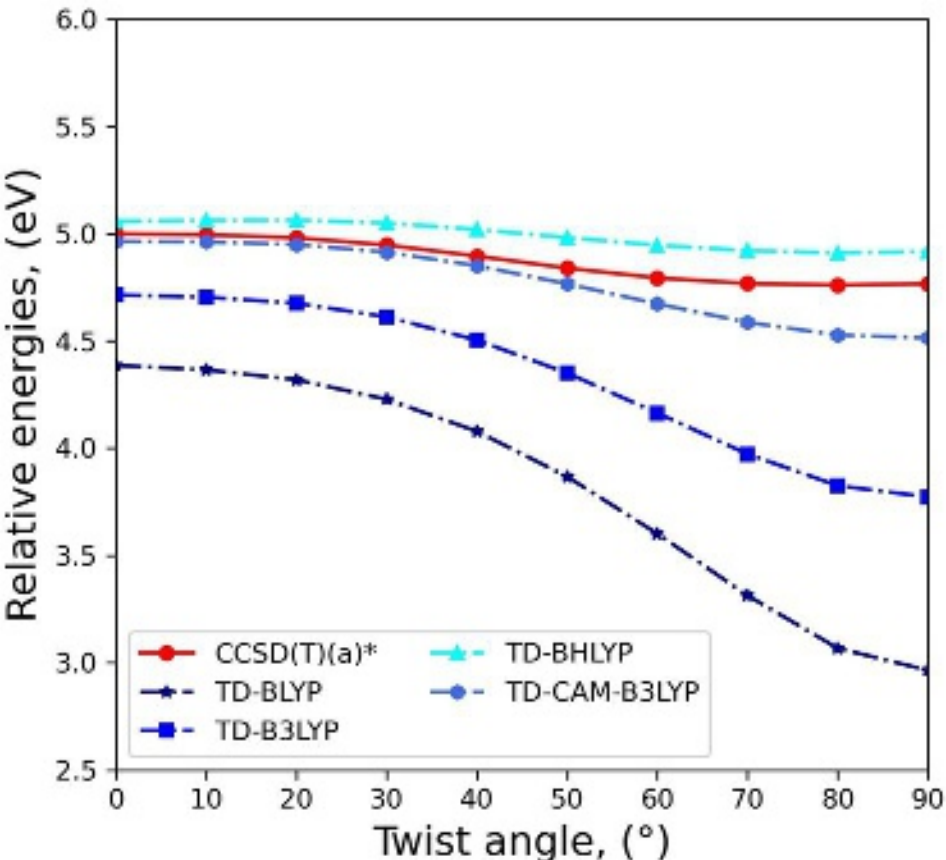
(c) CC2



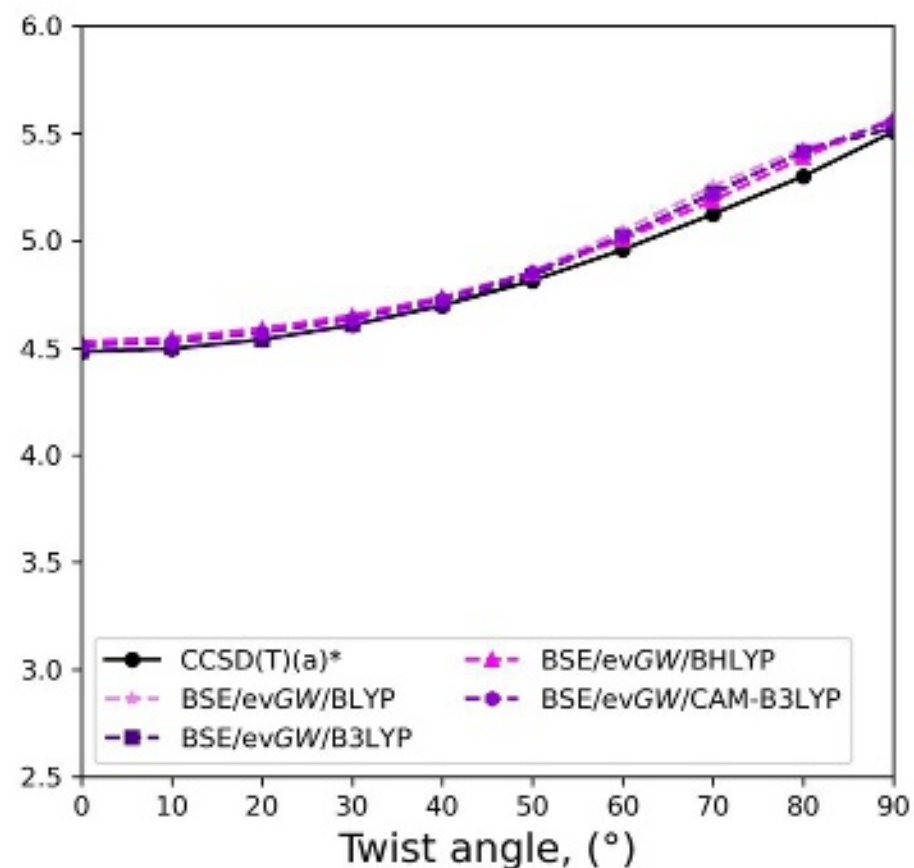
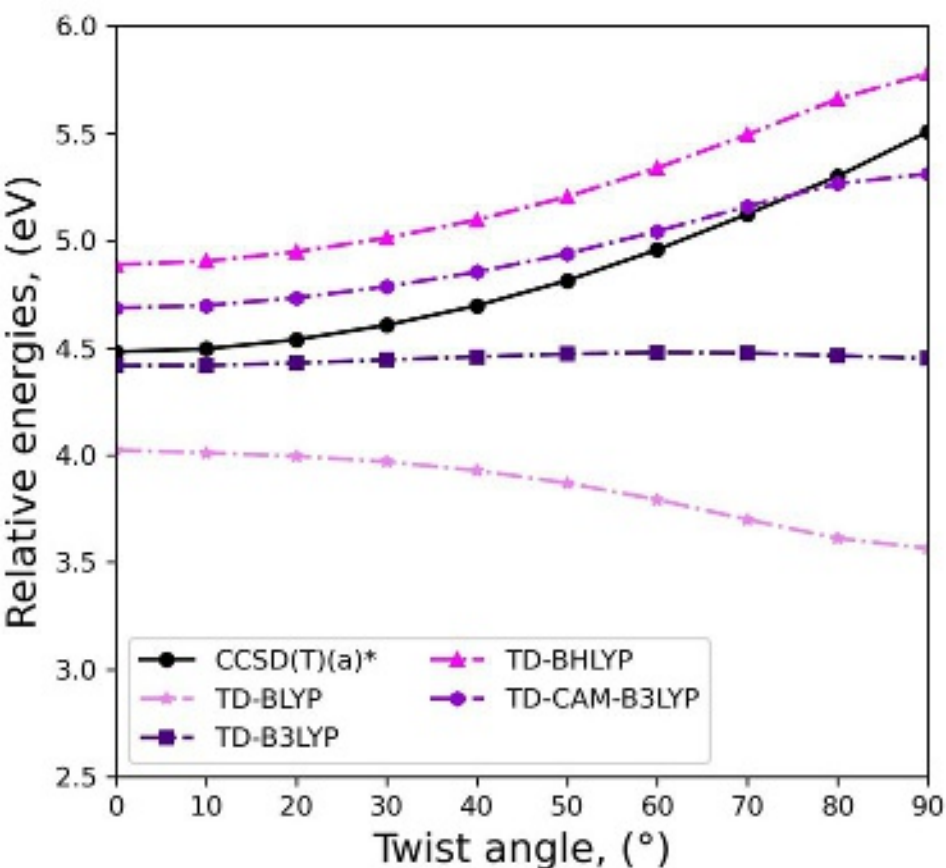
(d) TD-BLYP



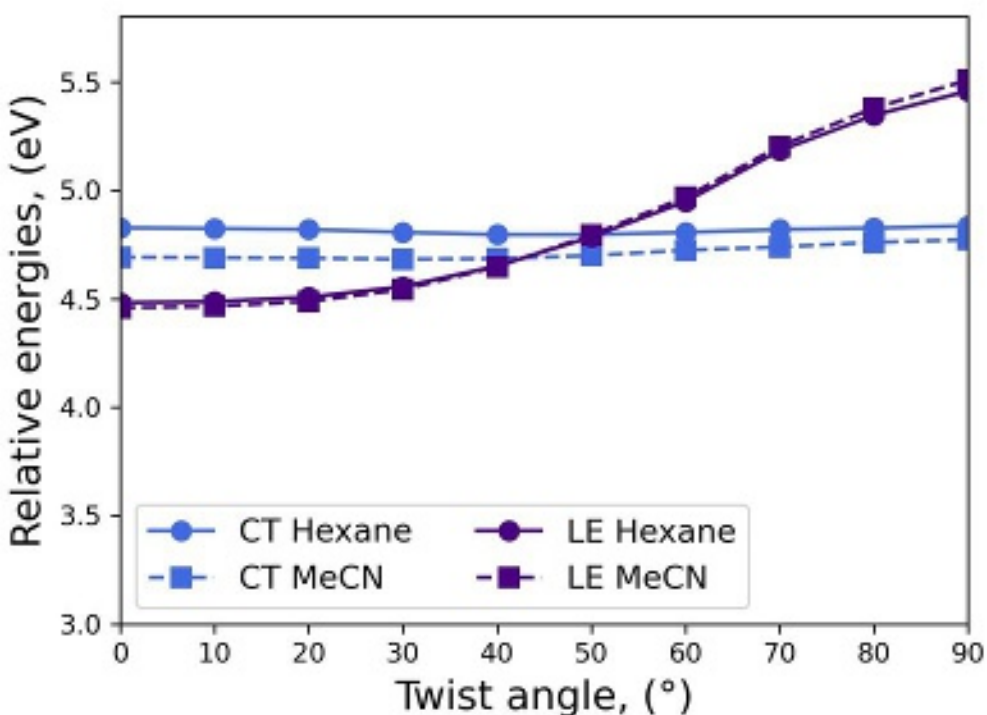
(e) BSE/evGW/BLYP



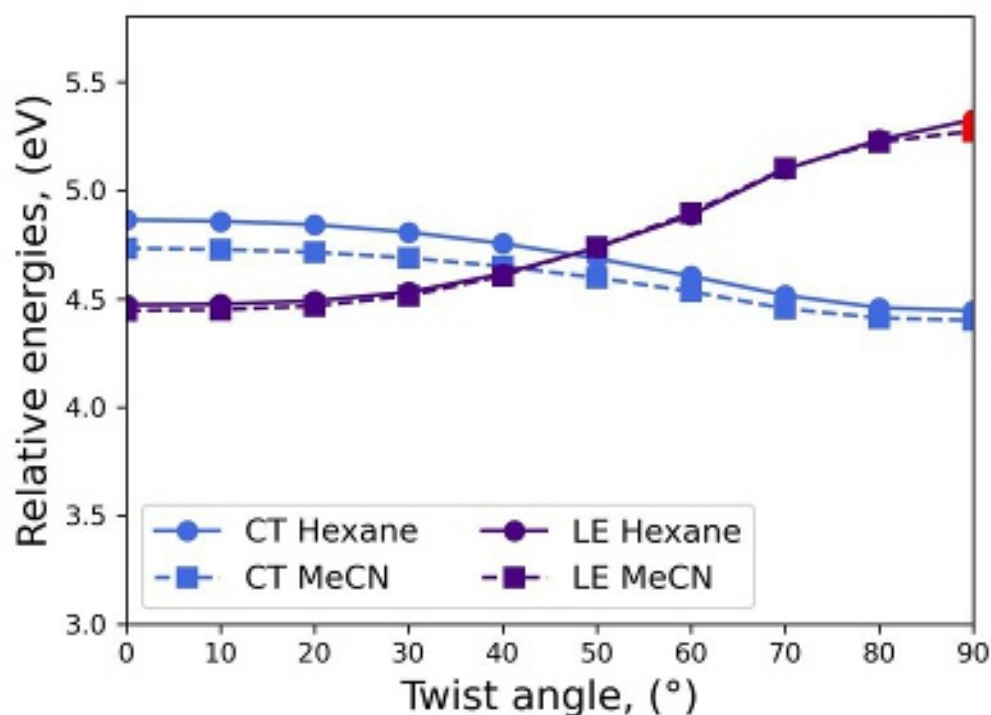
(a) CT state TD-DFT (left) vs BSE/evGW (right)



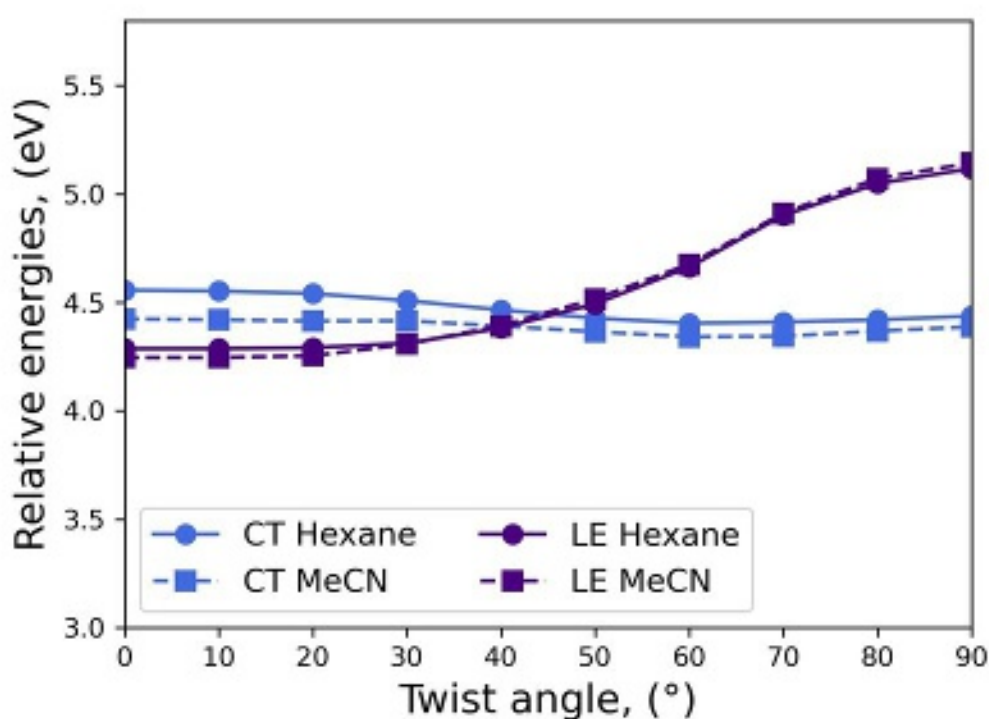
(b) LE state TD-DFT (left) vs BSE/evGW (right)



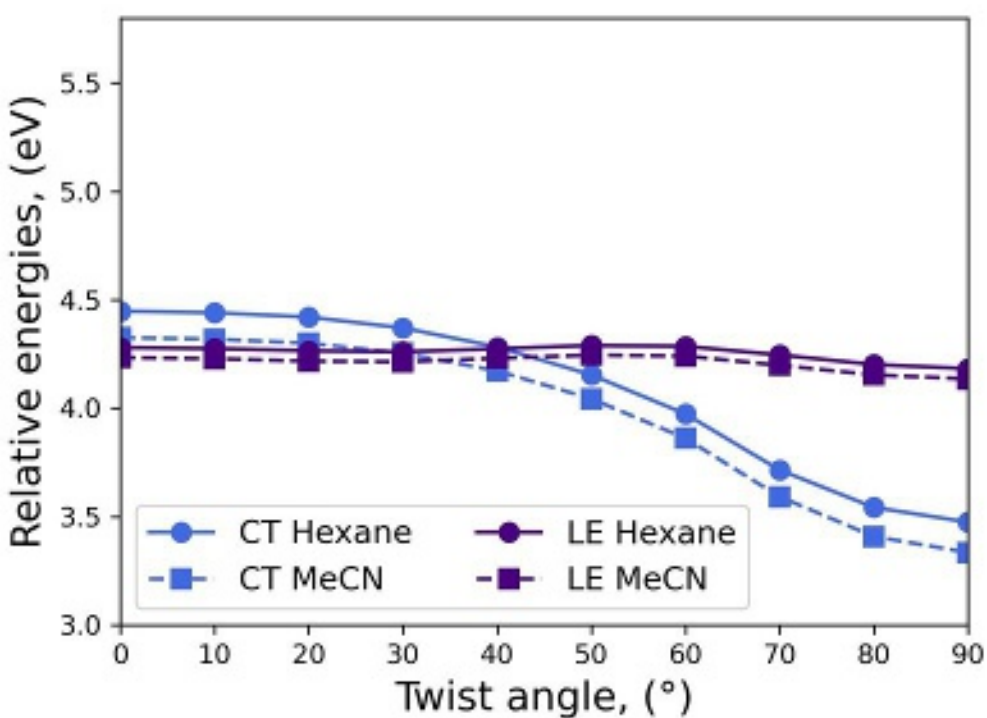
(a) LR-PTED-EOM-CCSD



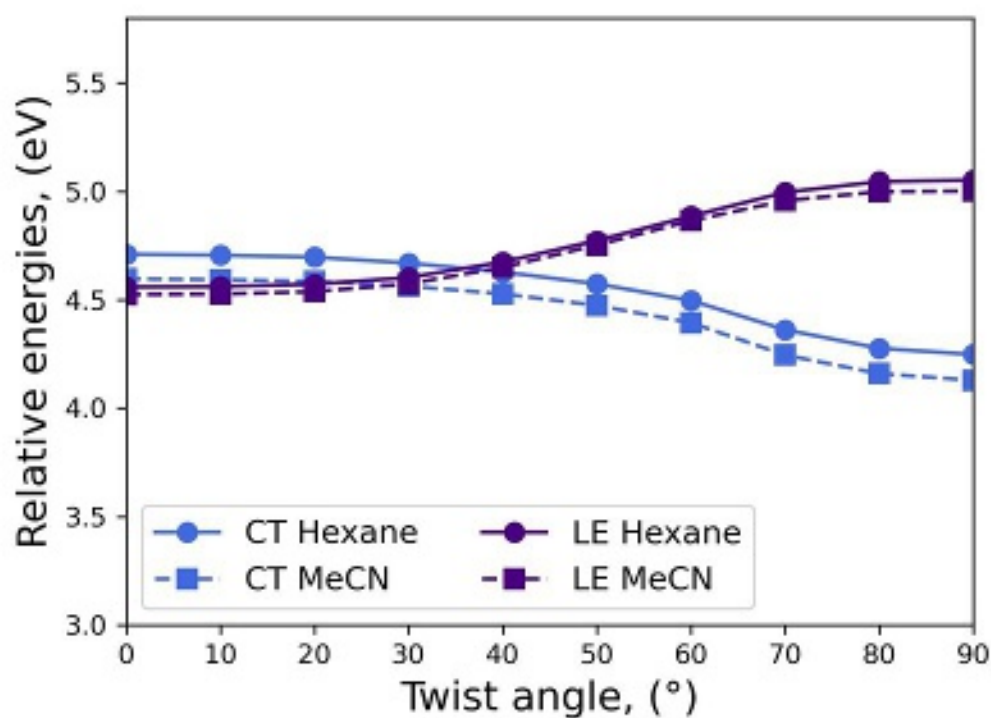
(b) SS-PTED-EOM-CCSD



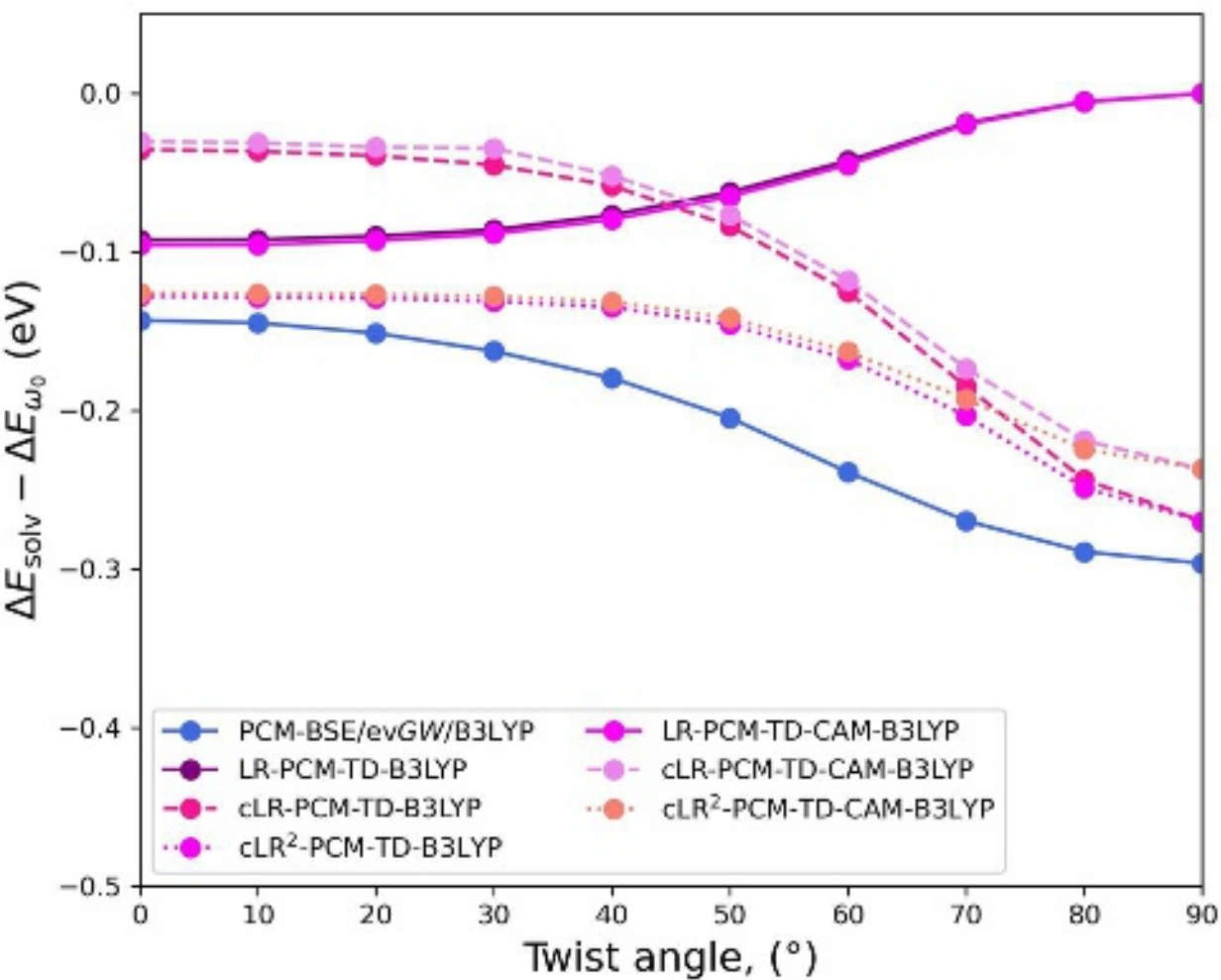
(c) PCM-BSE/evGW/B3LYP



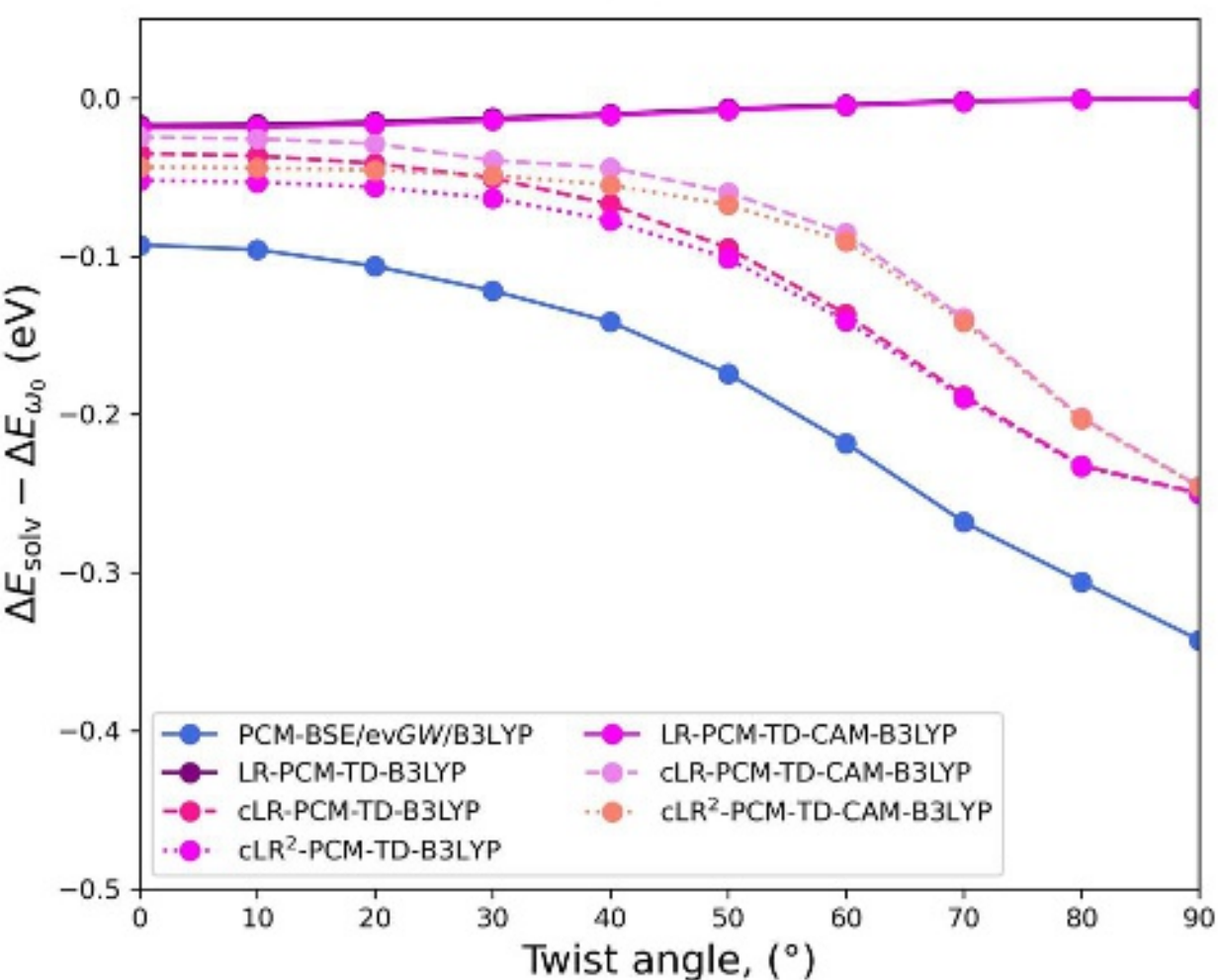
(d) cLR²-PCM-TD-B3LYP



(e) cLR²-PCM-TD-CAM-B3LYP



(a) CT



(b) LE

